...A 1524

april 1984

Instituut voor Cultuurtechniek en Waterhuishouding
Wageningen

PHYSICAL SOIL DEGRADATION:

ANALYSIS, MODELING AND EFFECTS OF SOIL COMPACTION DUE TO FIELD TRAFFIC IN MODERN AGRICULTURE

dr. A.L.M. van Wijk

Nota's (Notes) of the Institute are a means of internal communication and not a publication. As such their contents vary strongly, from a simple presentation of data to a discussion of preliminary research results with tentative conclusions. Some Notes are confidential and when so indicated are not available to third parties.

C O N T E N T S

1. INTRODUCTION

The research on physical soil degradation presented in this report has been sponsored by the CEC, DG VI, according to contract no. 0591 between CEC and the Institute for Land and Water Management Research, Wageningen, signed June 12th 1981. The research has been carried out over the period 1981 - 1983 in a joint project of four Dutch institutes:

- Institute for Land and Water Management Research (ICW), Wageningen
- Institute for Soil Fertility (IB), Haren
- Research Station for Arable Farming and Field Production of Vegetables (PAGV), Lelystad
- Agricultural University, Soil Tillage Laboratory (LH), Wageningen

This report summarizes in a more or less integrated form the contributions of the participating institutes to the project. Detailed information about theories and methods developed and results obtained can be found in the research papers and reports produced in the context of the project and listed at the end of each chapter.

1.1. Causes of physical soil degradation

During the latter 10-15 years general surveys in the field as well as complaints from practice revealed considerable physical soil degradation, occurring as a deterioration of soil structure and an increase of soil compaction reducing crop yield. In response to severe compaction yield depressions in order of 30 to 50% have been found. In the same time two developments could be observed in agriculture in the Netherlands: 1) an advancing mechanization with increasing wheel loads and 2) an intensification of crop rotation. To a great extent cereals have been replaced by root crops and silage maize, having a considerably greater mass to harvest at wetter soil conditions. At this moment more than 60% of the area of arable land in the Netherlands is used for growing potatoes (23%), sugar beets (18%) and silage maize (22%).

The advancing mechanization in agriculture is coupled with increasing

power and weights of tractors and capacities of lorries. The weight of tractors of 26, 92, 148 and 220 kW amounts to 2.1, 6.0, 9.6 and 12.0 tons respectively. About 1956 the highest capacity of a field lorry was 6 tons, nowadays 30 tons lorries are in use in agriculture. Trailed potato harvesters with hopper (two wheels) with a weight up to 5 tons and a hopper capacity of 5 tons and self propelled slurry carriers (three axles, six wheels) with weights of about 14 tons and a capacity up to 15 tons can be observed on arable fields. To reduce the ground pressures at these loads wheel equipments are adapted mainly by applying wider tyres. However, in spite of that soil compaction becomes ever more serious and extends to a depth beyond that of the annually main soil tillage, just for the wider tyre sizes.

In principle two options are open for the mechanized agriculture: 1) to continue the way taken and 2) to adapt mechanization and soil management systems. The first option implies accepting yield depressions due to compaction unless compaction is reversed regularly. In practice all kinds of rooters to loose the subsoil are applied ever more. This may point to favourable experiences of farmers with respect to the effectiveness of their soil loosening activities. However, there are also clear indications that the effectiveness has a restricted duration only especially in the case of light sandy loam and sandy soils. The second option starts from the prevention of soil compaction, but does not yet receive much interest from practice. This alternative could imply a restriction of wheel loads to a maximum limit, development of new wheel concepts or adaption of soil management systems by combining various field operations, greater working widths of implements or restricting field traffic to permanent lanes.

1.2. Objectives and scope of the research project

According to the objectives and the specific interests and experiences of the cooperating partners the project on physical soil degradation was subdivided into the following research topics covering processes, causes as well as effects of soil compaction:

1. Development of a mathematical model to predict soil compaction under wheels and experimental research to determine model parameters and data to verify model results.

2. Research on soil management systems and the relation between mechanization and soil compaction in practice.
3. Research of the relation between soil compaction and crop response.
4. Research of effects of climate and water management on soil compaction conditions.

In the present programme a first version of a model has been developed with the objective to obtain a tool that predicts the effect of different types of field traffic on soil compaction. Putting a heavy accent on practical applicability in this stage the model calculates soil compaction starting from a given rut depth. Supplemental field, laboratory and theoretical research has been carried out to support model development and to collect data for input in and verification of the model.

To examine the relation between mechanization, soil compaction and crop response different types of soil management systems comprising both controlled and uncontrolled field traffic experiments have been compared. Also an inventory of the relation between mechanization, field traffic intensity and -frequency and soil compaction was made in practice for different farm sizes and soil types.

The latter ten years a strong increase of the area of silage maize could be observed in the Netherlands. Silage maize is mainly grown on sandy soils in areas with a very intensive animal husbandry and therefore with an excess of slurry. This slurry is applied to a large extent on maize fields with tankers with ever more increasing capacities and wheel loads. To study the effects of heavy vehicle traffic on soil compaction and yield of silage maize long term experimental fields are started on different sandy soils.

In the context of the relation between soil compaction and crop response a theoretical study is made on rooting with special emphasis on root activity as far as affected by the soil - root contact.

In the present programme an existing and approved model that simulates soil moisture conditions in dependency of soil physical properties, rainfall and drainage conditions has been applied in the field of physical soil degradation research. It appeared that application of such models is very useful to investigate the influence of drainage on time and frequency of susceptibility to soil compaction on real time basis.

2. SOIL COMPACTION MODEL

2.1. Introduction

The extent to which a soil will be compacted during field operations depends on the type of field traffic as well as on the prevailing soil conditions. The pressures exerted to the soil by wheel traffic may vary widely depending on wheel properties (dimension, ply rating and inflation pressure of tyres) and wheel load. Moreover when loaded soils behave differently depending on the load, soil texture, bulk density and moisture conditions. However, it is not attainable to study the effects of all possible combinations of these factors in the field. Also the transferability of data obtained from experimental fields to other combinations of soil and traffic is often rather difficult. Therefore in addition to field studies there is a great need for tools that enable to study soil compaction at a wide variety of traffic and soil conditions. A model using both traffic and soil characteristics as input data is a valuable expedient to evaluate effects of various kinds of field traffic on soils at variable conditions. Such a model can be useful to examine the consequences of advancing farm mechanization and the possibilities of new wheel concepts in vehicle designing. In this chapter a model is presented that calculates the displacement of soil particles under wheel traffic and converts that displacement into a soil density distribution (VAN DE ZANDE and BOELS, 1984).

2.2. Principle of the model

In a given point (x,z) in a plane in the soil normal stresses (P) are acting, P_x in x-direction and P_z in z-direction. Perpendicular to the normal stresses shear stresses (τ) are operative indicated with τ_{xz} and τ_{zx} perpendicular to P_x respectively P_z (see Fig. 2.1).

Normal and shear stresses are not distributed uniformly. If in any point of the soil the forces and moments are in equilibrium (no rotation) and the influence of soil mass and acceleration forces are neglected, then holds:

$$\frac{dP_z}{dz} + \frac{d\tau_{zx}}{dx} = 0 \qquad (1)$$

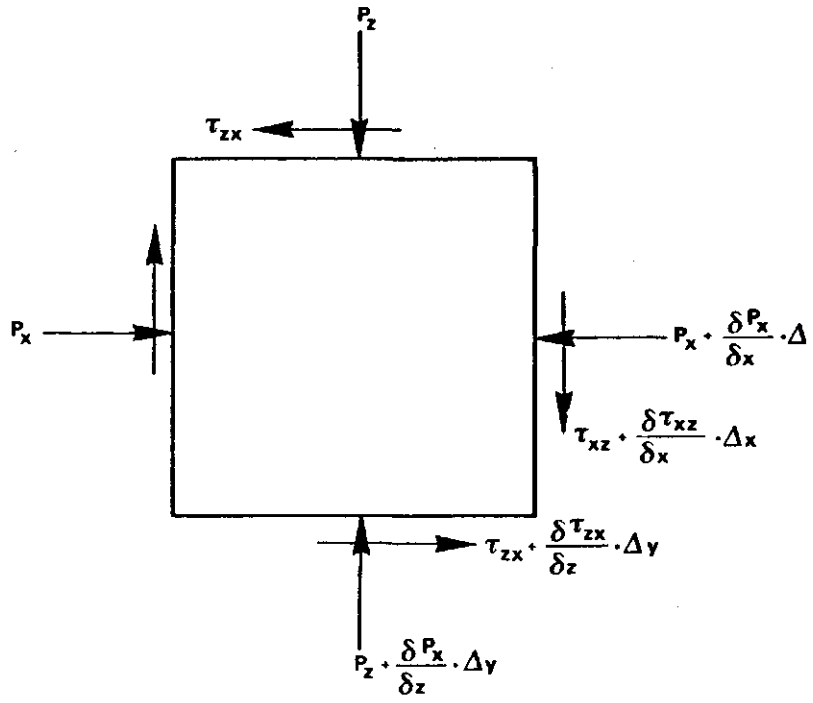

Fig. 2.1. Normal and shear stresses operative in an arbitrary plane in the soil

$$\frac{dP_x}{dx} + \frac{d\tau_{xz}}{dz} = 0 \qquad (2)$$

Stresses cause displacements in the soil medium. The displacement in the x-direction is indicated with u and in z-direction with v. After the elasticity theory the relation between displacement and stress can be written as:

$$\frac{dv}{dz} = (P_z - \upsilon P_x)/E \qquad (3)$$

$$\frac{du}{dx} = (P_x - \upsilon P_z)/E \qquad (4)$$

$$\frac{dv}{dz} + \frac{du}{dx} = \tau/K \qquad (5)$$

Explicitly written for P_x and P_z:

$$P_z = \frac{E}{1 - \upsilon^2}\frac{dv}{dz} + \frac{\upsilon}{1 - \upsilon^2} E \frac{du}{dx} \qquad (6)$$

$$P_x = \frac{E}{1 - \upsilon^2} \frac{du}{dx} + \frac{\upsilon}{1 - \upsilon^2} E \frac{dv}{dz} \tag{7}$$

Moreover it holds:

$$\frac{\partial \tau}{\partial z} = \left(\frac{\partial^2 u}{\partial z^2} + \frac{\partial^2 v}{\partial x \partial z}\right) K \tag{8}$$

$$\frac{\partial \tau}{\partial x} = \left(\frac{\partial^2 v}{\partial x^2} + \frac{\partial^2 u}{\partial z \partial x}\right) K \tag{9}$$

When eq. (6) is differentiated to z and eq. (7) to x and substituted together with eqs. (8) and (9) into eqs. (1) and (2), it is found:

$$\frac{E}{1 - \upsilon^2} \frac{\partial^2 v}{\partial z^2} + K \frac{\partial^2 v}{\partial x^2} + \frac{\upsilon}{1 - \upsilon^2} E \frac{\partial^2 u}{\partial x \partial z} + K \frac{\partial^2 u}{\partial z \partial x} = 0 \tag{10}$$

$$\frac{E}{1 - \upsilon^2} \frac{\partial^2 u}{\partial x^2} + K \frac{\partial^2 u}{\partial z^2} + \frac{\upsilon}{1 - \upsilon^2} E \frac{\partial^2 v}{\partial z \partial x} + K \frac{\partial^2 v}{\partial x \partial z} = 0 \tag{11}$$

where: E = modulus of elasticity

υ = poisson ratio

$K = \frac{E}{2}(1 + \upsilon)^{-1}$

v = vertical displacement (in z-direction)

u = horizontal displacement (in x-direction)

For solving the second order partial differential equations (10) and (11) proper boundary conditions have to be defined. The latter seems to be an insurmountable problem at this moment.

To be able to calculate soil compaction a simplification is applied assuming the soil as a quasi-elastic medium in which the major stresses are predominantly acting in vertical direction. That means P_x and τ_{xz} equal zero. For those conditions can be written:

$$\frac{\partial^2 v}{\partial x^2} + \frac{E}{K} \frac{\partial^2 v}{\partial z^2} = 0 \tag{12}$$

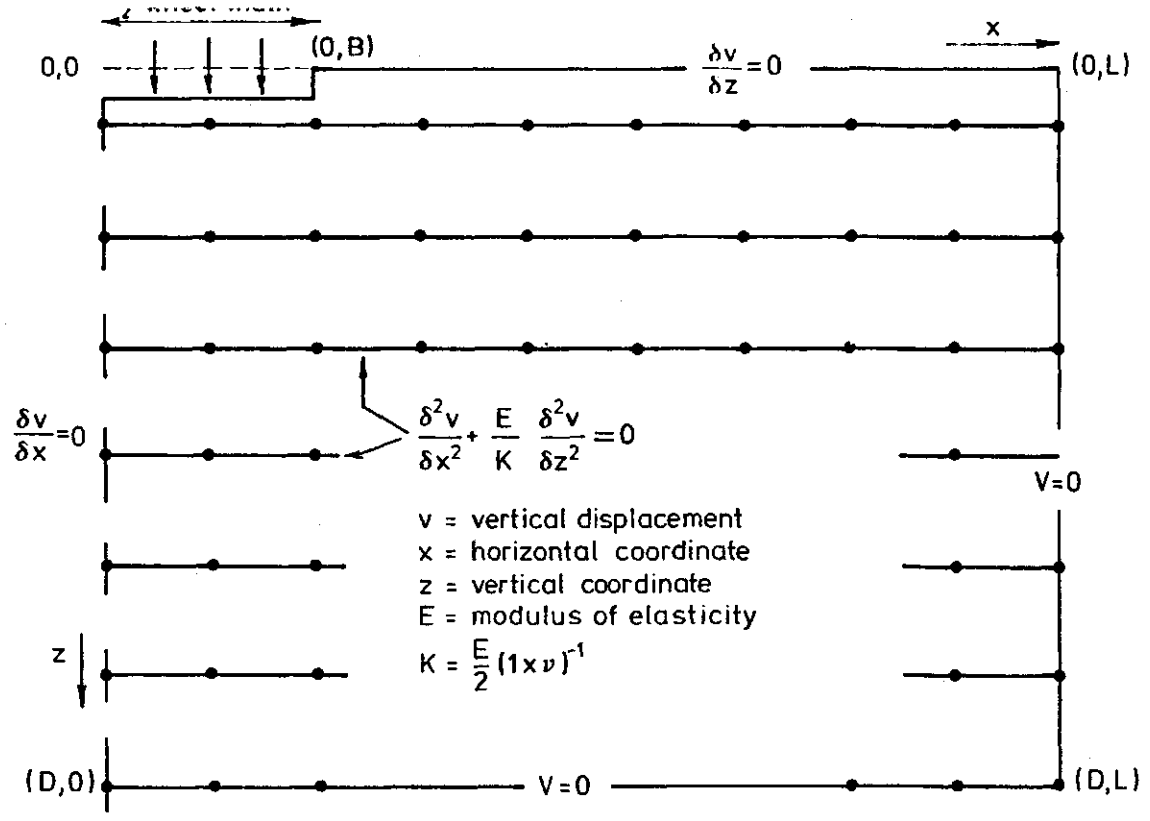

Fig. 2.2. Calculation scheme and boundary conditions of the compaction model

By solving numerically eq. (12) in each nodal point of a two-dimensional network perpendicular to the traffic direction the model calculates the displacement of soil elements under wheels starting from a prescribed rut depth (Fig. 2.2). The boundary conditions are:

at the top: - in the range (0,0) - (0,B) $v = f(z)$
- in the range (0,B) - (0,L) $P_z = 0$, then $\frac{\partial v}{\partial z} = 0$

at the bottom: - in the plane (D,0) - (D,L) $v = 0$

at the sides: - in the plane through the wheel-centreline $\frac{\partial v}{\partial x} = 0$
- in the plane (0,L) - (D,L) $v = 0$

2.3. Determination of model parameters

The differential equation (12) can be solved numerically when the two variables E and K are known, K is obtained from determination of the modulus of elasticity E and the poisson ratio υ. E is derived from uni-axial compression tests yielding the relation between bulk density and normal pressure. The latter can be converted to a relationship between normal pressure and sample height. The relationship between bulk density and normal pressure obtained with the uni-axial compression test

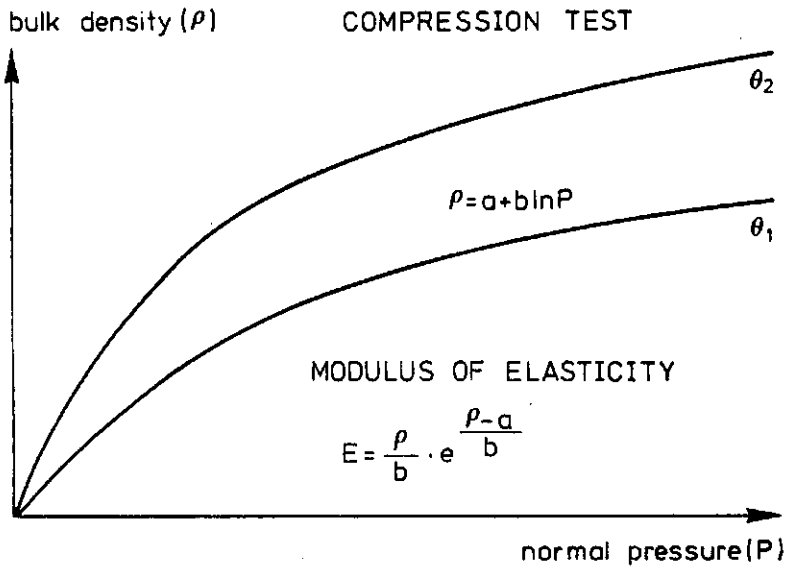

Fig. 2.3. Examples of bulk density - normal pressure relationships obtained from uni-axial compression tests

(Fig. 2.3) can be described after a logarithmic expression:

$$\rho = a + b \ln p \tag{13}$$

where: ρ = bulk density

a,b = soil constants depending on soil type and soil moisture content

p = normal pressure

The constants a and b can be found easy from a semi-logarithmic plot of bulk density versus normal pressure. The modulus of elasticity E is given by (law of Hooke):

$$E = \frac{p}{\varepsilon} \tag{14}$$

ε can be found from the relative change in height of a sample under compression:

$$\varepsilon = \frac{\rho - \rho_0}{\rho} \tag{15}$$

where: ρ_0 = initial bulk density

Instead of eq. (15) it can be written also:

$$\rho_0 = \rho - p \frac{d\rho}{dp}$$

so that holds:

$$\varepsilon = \frac{d\rho}{dp} = \frac{b}{p} \tag{16}$$

Combining eq. (14) with eqs. (13) and (16) the following expression is found for calculation of the modulus of elasticity:

$$E = \frac{\rho}{b} e^{\frac{\rho - a}{b}} \tag{17}$$

The second unknown variable K from eq. (12) is found by quantifying the poisson ratio υ in the expression:

$$K = \frac{E}{2} (1 + \upsilon)^{-1} \tag{18}$$

υ can be obtained from triaxial tests (see inset in Fig. 2.4). In the triaxial apparatus a soil sample enclosed in a cylindrical rubber membrane and at the top and bottom by rigid plates, is subjected to a normal pressure σ_1 applied through a loading ram to the top while supported by a surrounding radial pressure σ_3. During the test σ_1,σ_3,

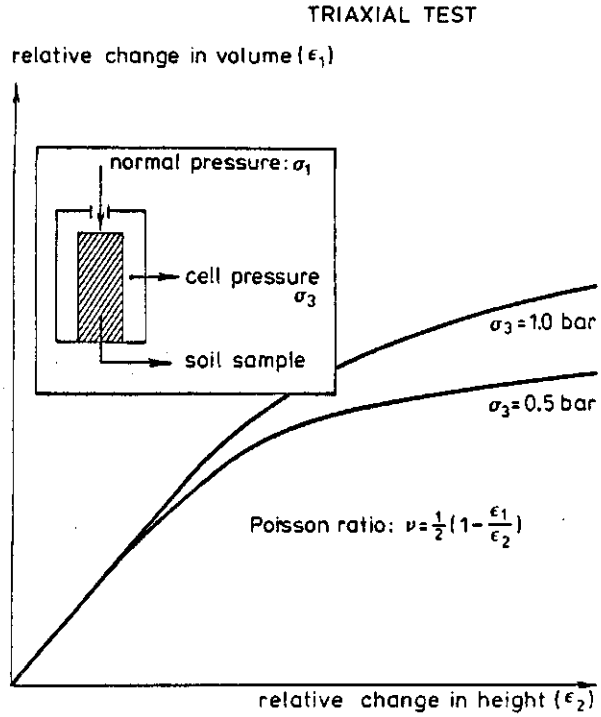

Fig. 2.4. Relationships between relative change in height and in volume obtained from the triaxial test. Principle of the triaxial test is given in the inset

relative change in volume (ε_1) and in height (ε_2) of the sample are registered. From those data υ can be found from:

$$\frac{\varepsilon_1}{\varepsilon_2} \frac{1}{1 - 2\upsilon} = \frac{\sigma_1 - 2\sigma_3}{\sigma_1 - 2\upsilon\sigma_3} \qquad (19)$$

Inserting the value of υ obtained from eq. (19) into eq. (18) the second unknown variable K from eq. (12) can be found.

The model does not take account of forces acting horizontally and so for displacement in horizontal direction. The poisson ratio υ has to be measured therefore at combinations of σ_1 and σ_3 approaching reality. It appeared that the absolute magnitude of ε_1 and ε_2 at small values of ε_2 are rather insensitive to the magnitude of the applied forces (see Fig. 2.4). Although not nice, the use of one value of υ becomes possible thereby.

2.4. Description of the program COMPAC

The program COMPAC calculates soil compaction under wheels, assuming a non-linear quasi-elastic soil behaviour. The program, written in FORTRAN IV calculates starting from a prescribed rut depth the displacement of nodal points in a network perpendicular to the wheel track (see Fig. 2.2). This network is subdivided horizontally in main layers and sublayers and vertically in main columns and subcolumns (see Fig. 2.5). The main layers and columns may differ in mechanical properties. From the displacement of the nodal points the change in bulk density of each element enclosed between four nodal points can be calculated. In the latter case a partly pure elastic behaviour is taken into account.

The program COMPAC consists of a main program that calls subsequently a number of subroutines.

Subroutine READIT

This subroutine asks input data about the object, the number of soil layers, the initial density, the constants a and b from eq. (13), place and depth of the wheel rut and data to arrange a grid system of main and sublayers and main and subcolumns.

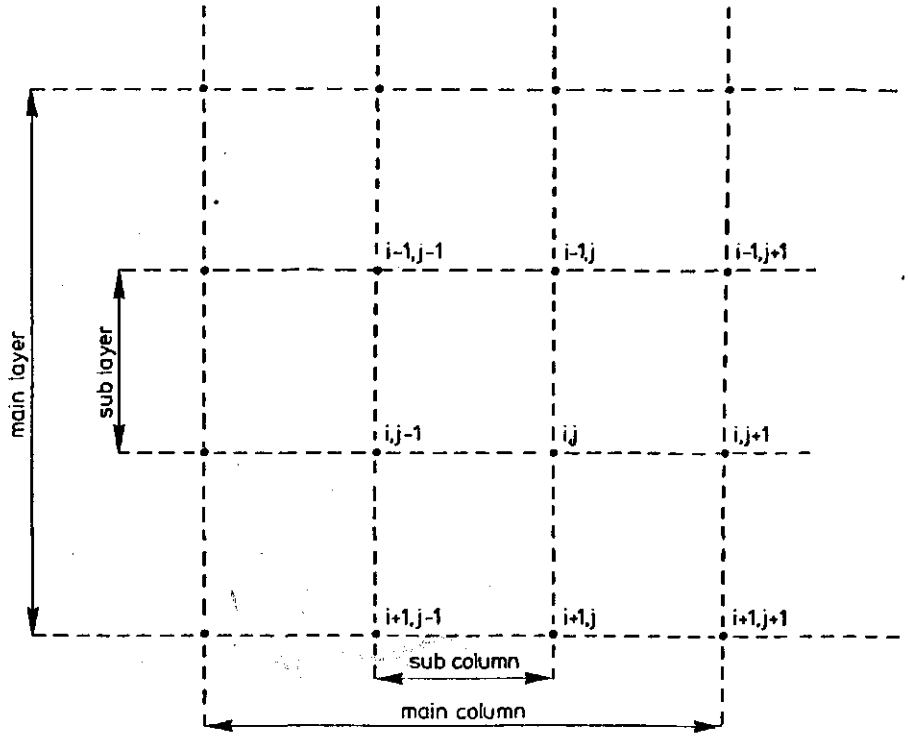

Fig. 2.5. Grid with nodal points, main and sublayers and main and sub-columns applied in the program COMPAC

Subroutine GRID

In this subroutine the grid is constructed from the data called by READIT. The x and z-coordinates of the nodal points are calculated and initial values of displacement and density are attached to each nodal point. From this subroutine other subroutines BOUND, RESIST, SOLVE, DENSIT and PRINT are activated for a number of times.

Subroutine BOUND

This subroutine defines place and width of the prescribed rut. Rut depth is increased stepwise to the final value.

Subroutine RESIST

This subroutine calculates elasticity moduli E in x and z-direction in dependency of the actual density in each nodal point. The vertical elasticity modulus (E_v) is determined with eq. (17) and represents the resistance against compression in vertical direction. To account for the resistance of shear along the edges of the adjacent subcolumns during vertical displacement a horizontal elasticity modulus is computed in

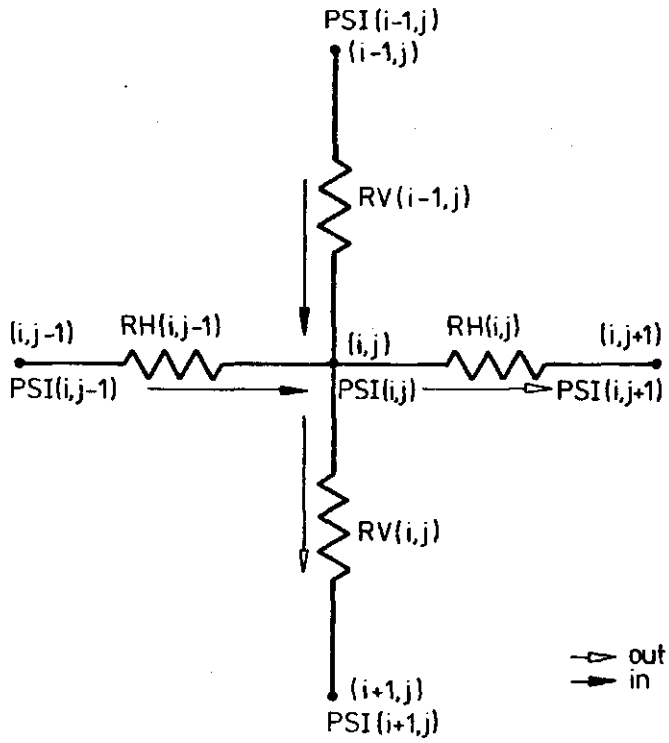

Fig. 2.6. Calculation scheme of displacement of the nodal points

each nodal point as an averaged of the coefficients of the layers above and below that nodal point:

$$E_{i,j} = (EUP + ESUP)/2$$

where: $EUP = (z_i - z_{i-1}) \times \upsilon \times E_{i-1,j}$

$ESUP = (z_{i+1} - z_i) \times \upsilon \times E_{i+1,j}$

Subroutine SOLVE

Starting from the prescribed displacement of the nodal point in the rut this subroutine calculates displacements in each nodal point of the grid using equations describing a quasi-elastic soil behaviour. The procedure of the calculation in each nodal point is schematized in Fig. 2.6. The calculation of the new state in the nodal point starts from an equilibrium between input deformation to and output deformation from that nodal point.

Deformation to the point (input) is:

$$RH(i,j-1)\{PSI(i,j-1) - PSI(i,j)\} + RV(i-1,j)\{PSI(i-1,j) - PSI(i,j)\} \quad (20)$$

from the point (output):

$$RH(i,j)\{PSI(i,j) - PSI(i,j+1)\} + RV(i,j)\{PSI(i,j) - PSI(i+1,j)\} \quad (21)$$

where: PSI = displacement
RH resp. RV = resistance in horizontal resp. vertical direction
(i,j) = grid coordinates

It holds in = out or in - out = 0, yielding the equation:

$$RH(i,j-1) \cdot PSI(i,j-1) + RV(i-1,j) \cdot PSI(i-1,j) +$$
$$RH(i,j) \cdot PSI(i,j+1) + RV(i,j) \cdot PSI(i+1,j) -$$
$$\{RH(i,j-1) + RV(i-1,j) + RH(i,j) + RV(i,j)\} \cdot PSI(i,j) = 0 \quad (22)$$

Eq. (22) is first solved in the direction of the rows to find PSI(i - 1,j) and PSI(i + 1,j). The equation to solve becomes then:

$$RH(i,j-1) \cdot PSI(i,j-1) - \{RH(i,j-1) + RV(i-1,j) + RH(i,j) +$$
$$RV(i,j)\}PSI(i,j) + RH(i,j) \cdot PSI(i,j+1) = -RV(i-1,j) \cdot PSI(i-1,j) -$$
$$RV(i,j) \cdot PSI(i+1,j) \quad (23)$$

To facilitate the calculation, eq. (23) is split up into a set of four equations which are solved in each nodal point with the Gauss' elimination method:

$$COEF(i,1) = RH(i,j-1) \quad (24a)$$

$$COEF(i,2) = -\{RH(i,j-1) + RV(i-1,j) + RH(i,j) + RV(i,j)\} \quad (24b)$$

$$COEF(i,3) = RH(i,j) \quad (24c)$$

$$RHS(i) = -RV(i-1,j) \cdot PSI(i-1,j) - RV(i,j) \cdot PSI(i+1,j) \quad (24d)$$

Then the same procedure is applied in the direction of the columns yielding PSI(i,j - 1) and PSI(i,j + 1).

Subroutine DENSIT

This subroutine calculates the new bulk density per layer and column from the initial density and displacement found with SOLVE. Requiring that there is no loss of mass from the columns the new density is found with:

$$RHO(i,j) = INITRO(z_1)/\{1 - PSI(i,j) - PSI(i+1,j)/z(i+1,j) - z(i,j)\}$$

where: RHO = new bulk density
INITRO = initial bulk density
z = vertical coordinate

Subroutine PRINT

This subroutine tabulates the output data about displacement and bulk density.

2.5. Verification of the model

To test the model a number of controlled traffic experiments were carried out in a soil bin. This bin has a length of 4 m and a width and height of 0.6 and 0.5 m respectively and was filled with a sandy loam soil (about 20% of the particles <16 μm). The soil in the bin was compacted to a bulk density of about 1.30 $g \cdot cm^{-3}$. The moisture content amounted to 16%. The soil was subjected to wheel pressures using a rigid steel wheel with a width of 10 cm and a diameter of 48 cm. The number of wheel passes varied from 1 to 6. With the aid of markers placed previously in a grid of 2 x 2 cm into the soil both the horizontal and vertical displacement of soil particles under the wheel could be established.

Also the vertical displacement has been computed with the model starting from the rut depth measured in the soil bin experiments. To this end the next values of the soil parameters were derived for the soil in question: a = 1.469, b = 0.147 and υ = 0.350 (see Section 2.3). The model calculation started from the same initial bulk density as applied in the soil bin experiments.

Fig. 2.7 compares the vertical displacement of soil elements under the rut computed by the model (left part) and measured in the soil bin (right part). In the region right below the wheel the computed displacements correspond rather well with those measured. With increasing depth the model overestimates the vertical displacement a little (see Fig. 2.8a). When the vertical displacements are converted to bulk densities and pore volumes (see Fig. 2.8b) the model results appear to approach the measured data rather well. The model calculation yields pore volumes which differ only about 1.5% from the measured ones.

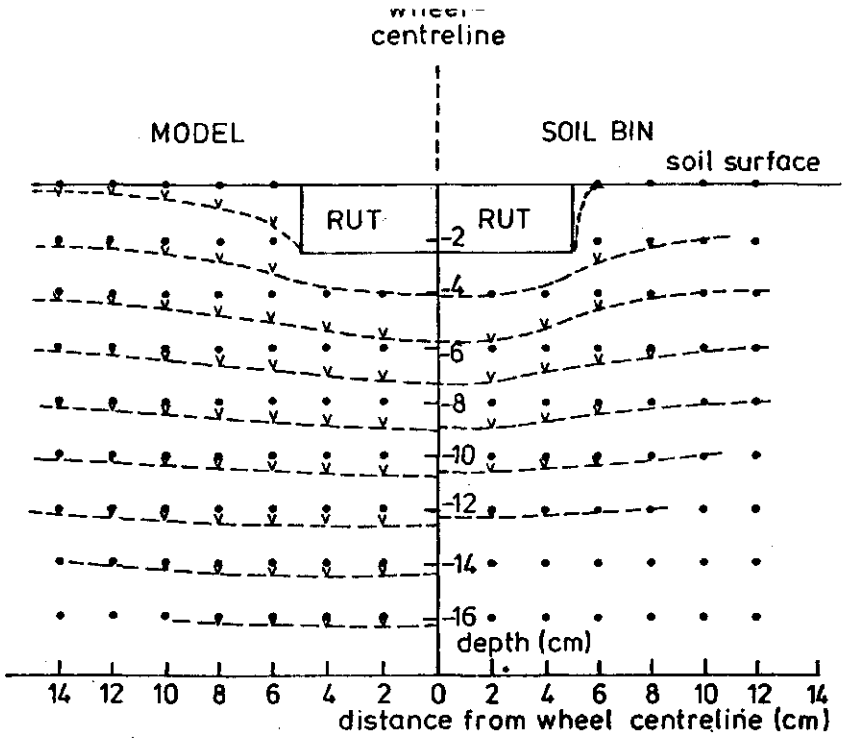

Fig. 2.7. Comparison of simulated (left) and measured (right) soil displacement under a wheel

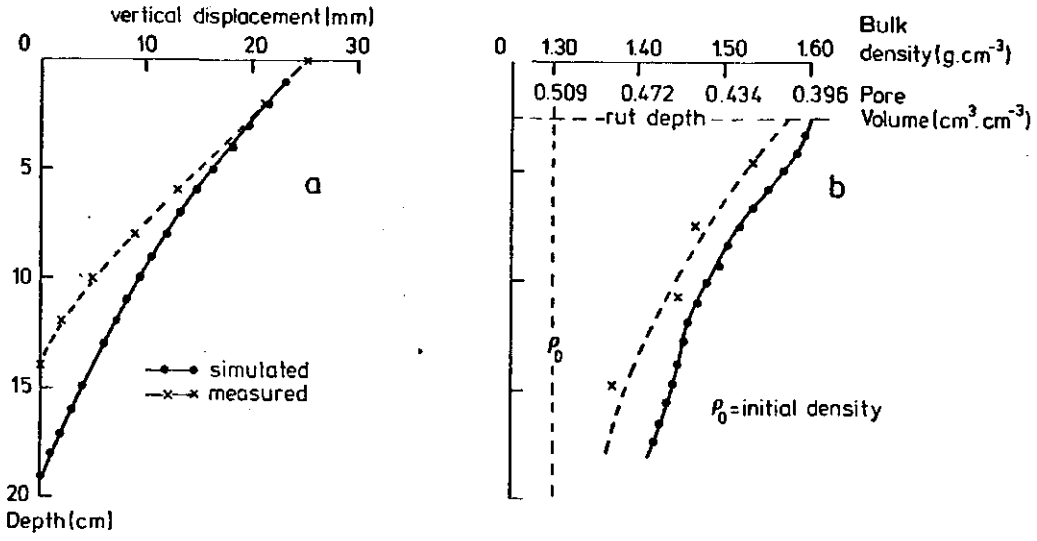

Fig. 2.8. Distribution of simulated and measured vertical displacements under the wheel centreline (a) and of bulk density and pore volume (b) converted from the displacements

In the region beside the rut the agreement between computed and measured displacements is less. The rut in the soil bin has rather sharp edges, while in the model simulation the soil surface beside the wheel sinks over a rather wide distance from the wheel. The latter phenomenon

will occur only during loading of longer duration. Moreover in practice just an upheavel near the wheel track is often found as a result of plastic deformation of the soil.

However, in practice the main interest goes to the maximal compaction to be expected under wheel traffic. This maximal compaction occurs in the region immediately under the wheel track. In spite of deviations of model results directly beside the wheel rut the model is useful to predict the maximum soil compaction with a rather good accuracy.

2.6. Comments to the present version of the model

This study has to be considered as an introduction into the field of modeling the rather complicated soil mechanical processes governing compaction of soil under wheels. In an attempt to develop a model that can be applied to practical problems in the first place, in the present state of the study a heavy accent is put on the practical applicability of the model. This includes also the simplicity of determination of the required input parameters. The model starts from a prescribed rut depth exactly to measure in the field. Moreover it uses soil parameters that can be obtained from rather simple and generally available uniaxial compression tests and triaxial tests. In its present state the model calculates rather well soil compaction right under wheels from track depths obtained from artificial wheel traffic in controlled soil bin experiments. Soil compaction measured in controlled experiments as well as simulated with the model decreases gradually with depth. However, the model calculation starts from a prescribed depth of tracks, what restricts the predictive power of the model to situations afterwards. To overcome this restriction and to make the model more useful for practical application the model has to be extended and adapted, in such a way that the stresses acting in the soil - wheel contact surface form the point of departure of the model computation. These stresses which depend on soil conditions and type of traffic (wheel dimensions, wheel loads and inflation pressure) induce a spatial distribution of stresses in the soil medium below the wheel. This stress distribution can be converted to a density distribution on basis of experimentally determined density - stress relationships. This approach requires supplemental research (i) on mathematical description of the spatial stress field under wheels starting from the stress distribution in the soil - tyre

contact surface; (ii) on relationships between stress and bulk density from compression tests for different soil types and soil moisture conditions; (iii) to collect input data for the model i.c. stress distributions in the soil - tyre contact surface for different types of field vehicle traffic and (iv) to measure compaction patterns under wheel tracks in the field to verify model results.

In the present programme field traffic frequencies and -intensities could be visualized in the form of rut patterns with known tyre dimensions, tyre inflation pressures and wheel loads, all in connection with farm size and type of crop (see Chapter 4). These data coupled with the stress distributions in the soil - tyre contact surface to determine in the supplementary research will enable a model calculation of seriousness of soil compaction in intensive farm systems.

2.7. Reports and papers

HAVINGA, L. and D. BOELS, 1982. Compaction of a sandy soil due to different wheel loads (Dutch). Nota ICW 1388. 40 p.

ZANDE, J. VAN DE and D. BOELS, 1984. A two-dimensional model for calculation of soil compaction under wheels (Dutch). Nota ICW (in preparation).

3. RESEARCH IN SUPPORT OF MODEL DEVELOPMENT AND APPLICATION

3.1. Soil parameters

Basically, the model uses a soil stress - bulk density relationship that is the result of a so-called uni-axial compression test. In this test a downward moving piston compresses soil in a cylinder (Fig. 3.1). By measuring the mean pressure on the piston (σ_1) and the soil porosity (P) continuously during the test, a σ_1 - P relationship can be determined. The lateral strain is zero and the σ_3/σ_1 ratio is usually about 0.5. When the direction of movement of the compacting piston is reversed a small but significant elastic rebound of the soil occurs. As soon as the soil is fully unloaded, the soil starts to expand (creep) at a very low and ever decreasing rate, but a true condition of rest is never reached. The results of the test depend primarily on soil type, moisture content, and rate of loading (piston speed), but more factors are important. The aspects mentioned in the Sections 3.1.1 to 3.1.4 have been investigated applying the uni-axial compression test.

3.1.1. Soil behaviour in repeated loading

Lexkesveer loam was uni-axially compressed to σ_1 = 4 bar and unloaded. This loading cycle was not, or 4 or 14 times repeated (Fig. 3.2). It appeared that after 15 loading cycles the soil was still further

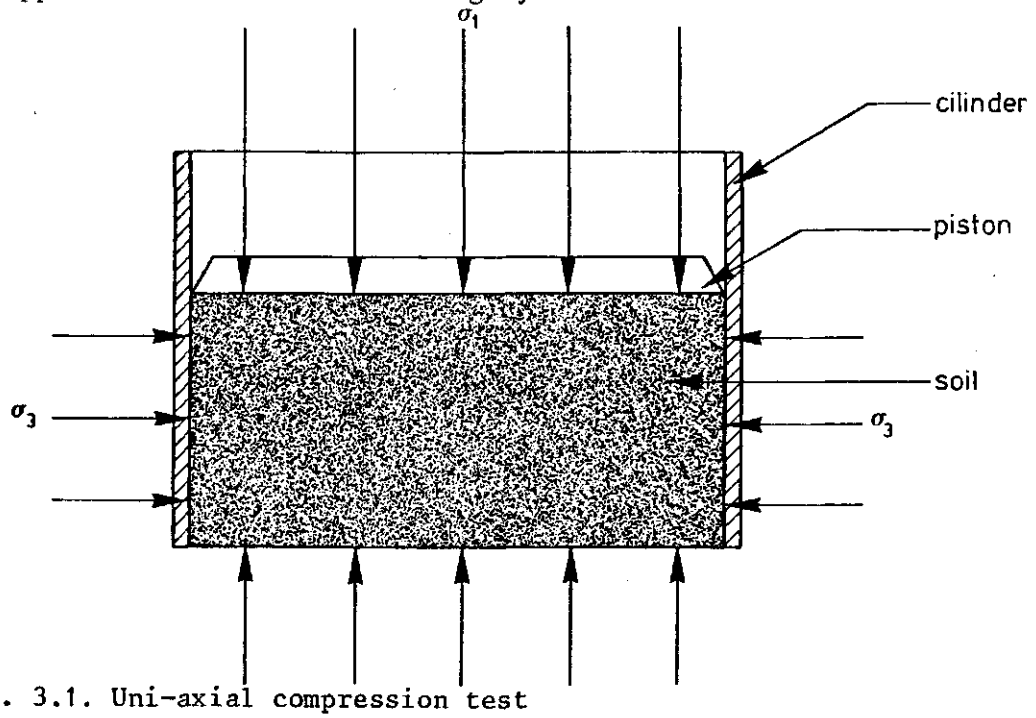

Fig. 3.1. Uni-axial compression test

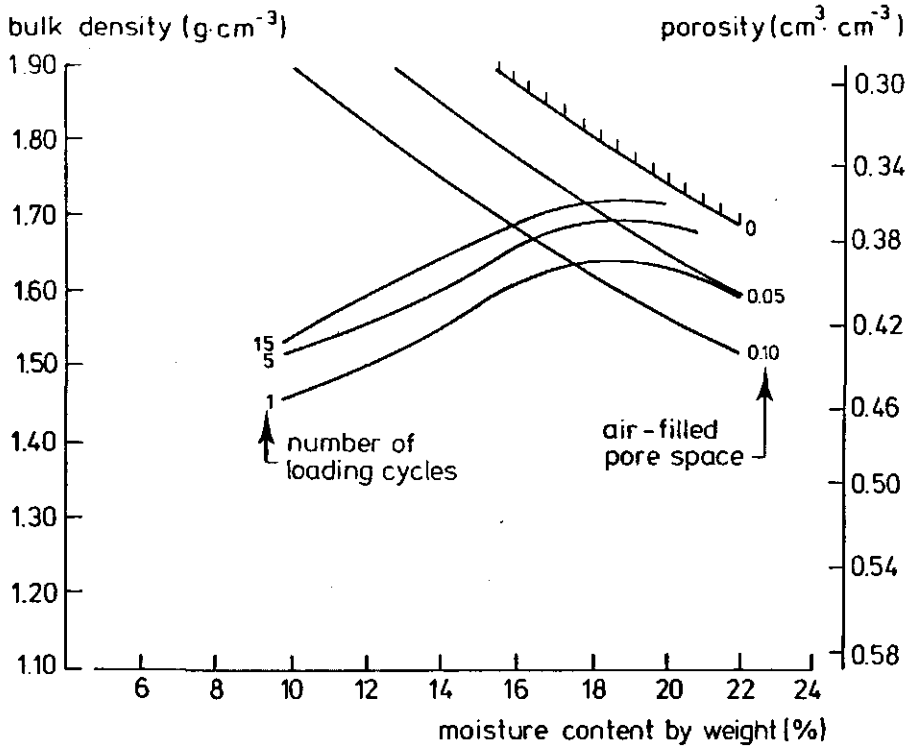

Fig. 3.2. Soil behaviour in repeated loading

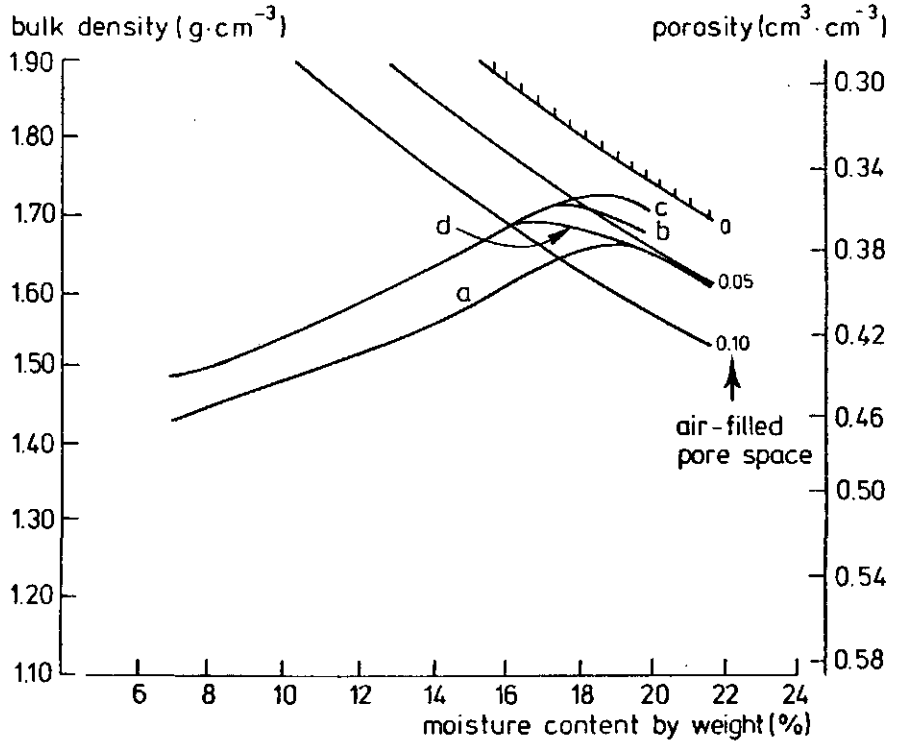

Fig. 3.3. Soil behaviour in repeated loading with additional treatments: a and b, 1 resp. 15 loading cycles; c, 15 loading cycles and 4 rest periods; d, idem c with drying and rewetting

compacted in repeated loading. A rest period of 3.5 or 7 days after each three loadings made the soil more compactible under moist conditions, but not under conditions drier than a moisture content of 16% (Fig. 3.3). Drying and rewetting of the sample during a rest period of 7 days, on the other hand, decreased compactability. Here again the effect was only present at moisture contents >16% (HOFSTRA, 1982).

3.1.2. Influence of aggregate size

Compaction generally starts in a loose bed of soil aggregates of different sizes with a certain aggregate size distribution. It appeared that the absolute values of the sizes do not influence compactability. The size distribution, however, affects compactability, but its influence diminishes when the state of compaction increases.

3.1.3. Creep and soil air effect in elastic rebound

When soil is compacted to low values of air filled pore volume, it frequently happens that air becomes entrapped and air pressure builds up. In unloading, this compressed air makes soil exhibit a very large elastic rebound. This phenomenon was investigated for a loam, a clay,

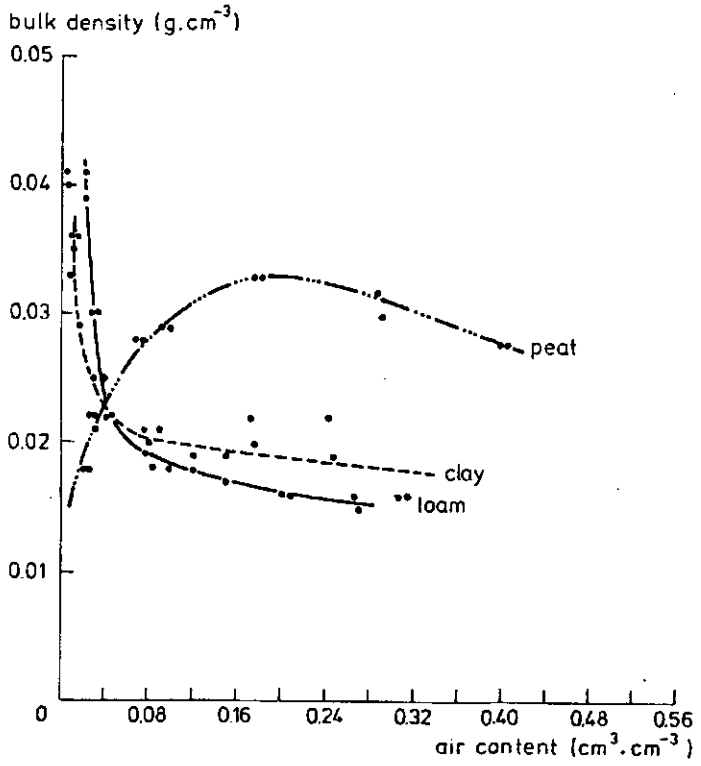

Fig. 3.4. Bulk density after compaction to 4 bar and unloading for soil samples with different moisture contents

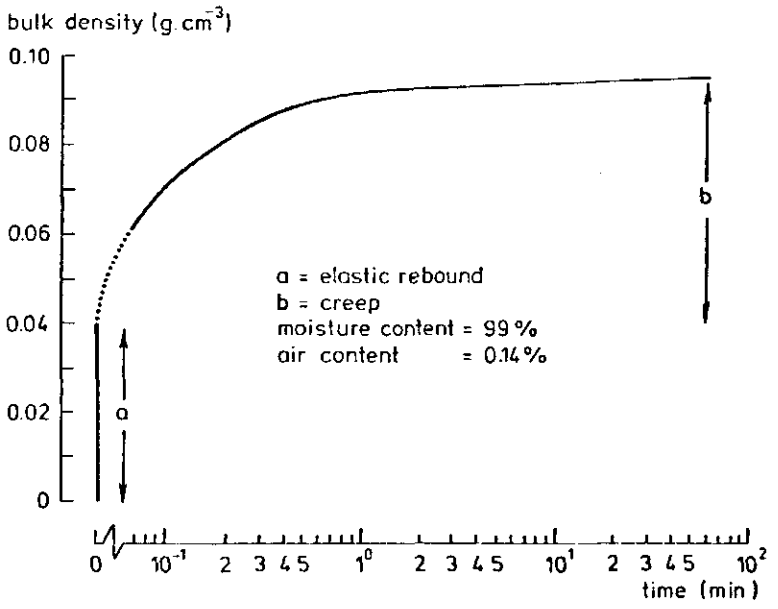

Fig. 3.5. Behaviour of peat soil in and after unloading

and a peat soil through uni-axial compression tests to σ_1 = 4 bar, followed by unloading, on soil samples with different moisture contents from moist to rather wet (Fig. 3.4). Due to air expansion the bulk density increases up to 0.04 g·cm^{-3} when the loam and clay are unloaded.

Peat behaves different: here air is forced out of the water filled continuous pore system. The load is for a greater part carried by the soil water when moisture contents are high. Water cannot contribute to the rebound, which means that rebound of wet peat decreases with increasing moisture content. The elastic rebound of peat that is not in a wet condition is large (up to 0.04 g·cm^{-3}). In peat creep can be more important than elastic rebound. Fig. 3.5 shows a total creep value of 0.05 g·cm^{-3}. Loading speed affected elastic rebound only in the peat; when speed is increased, rebound also increases (SWINKELS, 1982).

3.1.4. Time effects on soil water pressure after compaction

Soil compaction, on a micro-scale, is a rather chaotic process. It means that, immediately after a compaction process, the soil water is chaotic distributed and pressure varies from point to point in the soil water. But as soon as compaction is stopped, an equilibrating process starts tending to a uniform soil water pressure value all over the sample. It involves transport of water on a micro-scale, which takes time. Due to the above, soil water pressure measuring values change with time after compaction until an equilibrium value is reached. It is

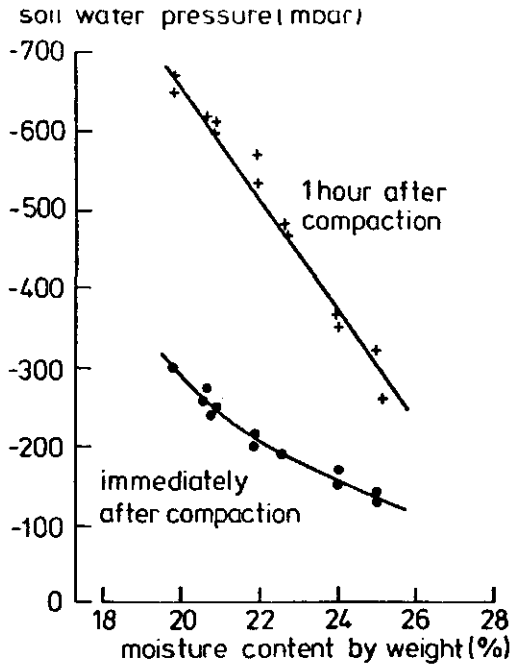

Fig. 3.6. Time effects of water pressure in Wageningen silty clay loam after compaction

illustrated in Fig. 3.6. As soil water pressure is one of the factors that determine soil strength, soil strength also changes with time after compaction (DAMIAN, 1983).

3.2. Conditions in the soil - wheel contact surface

On behalf of the further development of the model and the increase of its applicability information is needed on phenomena that influence the stresses in the wheel - soil contact surface. To this end attention is paid to the following aspects:

- rut depth, and the accompanying largest σ_1-values that have ever acted on a rut section perpendicular to the direction of travel;
- the (effective) directions of these stresses;
- load duration, as the pertinent soil parameters are highly dependent on loading speed for a large class of soils;
- backward displacement of the soil at the rut surface. This displacement causes distortions within the soil mass. It seems that large distortions increase soil porosity slightly, but are detrimental for the soil structure as well. It may be necessary to include these phenomena in the model.

3.2.1. Largest principal stresses across the rut width

To evaluate the largest principal stresses (σ_1) that ever acted across the width of a rut, two approaches have been followed: (i) desk research of relevant literature and compilation of existing knowledge in this area in a book (KOOLEN and KUIPERS, 1983) and (ii) development of an indirect measuring method.

As it is very difficult to measure σ_1-values directly when tyres both flatten and show sinkage into the soil, being the interesting case, a method has been developed to measure σ_1-values indirectly (Fig. 3.7).

- With a tyre, a rut is formed, along a cross section of which the distribution of the largest σ_1-values that have ever acted on the surface is wanted to be determined (see Fig. 3.7a).
- At the same time 3 plate impressions are made in the neighbourhood of the rut, to mean normal contact - stresses of 1, 2 and 4 bar re-

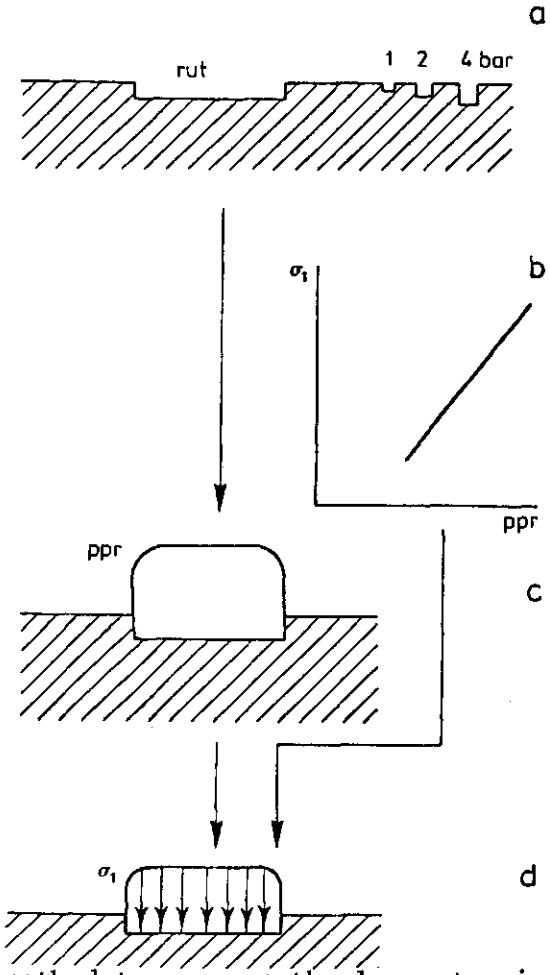

Fig. 3.7. Indirect method to measure the largest principal stresses (σ_1) occurring across the width of a rut (ppr = pocket-penetrometer reading)

spectively. The plate used is rigid, very smooth, and has a diameter of 20 cm. Impression speed is selected such that compaction rates are the same under the plate and the tyre (see Fig. 3.7a).

- Using a hand-operated micro-penetrometer (the Soil-Test pocket penetrometer) a number of pocket-penetrometer readings (ppr) are made according to a certain pattern in each bottom of the three plate holes and a representative ppr for each hole is calculated.
- Plotting these three calculated ppr against the mean normal contact stress under the plates, a calibration graph is obtained, which allows to estimate the largest σ_1 that has ever acted on a surface element of that particular soil from pocket-penetrometer readings (ppr) taken in that surface element (Fig. 3.7b).
- Simultaneously many ppr are taken in the bottom of the rut and the ppr-distribution across the width of the rut is determined (Fig. 3.7c).
- Using the calibration graph, this distribution is translated into a σ_1-distribution (Fig. 3.7d).

The method is being tested at the moment and the first results are encouraging. It is hoped that the method is able to cope with heterogeneous field conditions and is insensitive to vertical moisture variations in the soil profile.

Basically, the method utilizes the following general relationships:

- for a given soil type at a given moisture content, porosity is mainly determined by the largest σ_1 that has ever acted;
- for a given soil type at a given moisture content, penetration resistance is mainly determined by porosity.

3.2.2. Tyre inflation pressure

Tyre inflation pressure is one factor that determines soil - wheel contact stresses. To get information on the actual tyre inflation pressures at which agricultural operations are performed, inflation pressures are measured for many tractor-plow combinations on Dutch clay soils in 1980 (DEN HAAN, 1981; TIJINK en DEN HAAN, 1981). Results are given in Fig. 3.8. As the differences between left and right were small, only pressures of the right tyres have been given. Measured inflation pressure of the rear tyres ranges from 0.6 to 3.0 bar. There is a clear peak between 1.2 and 1.4 bar. In 55% of the cases rear tyre inflation

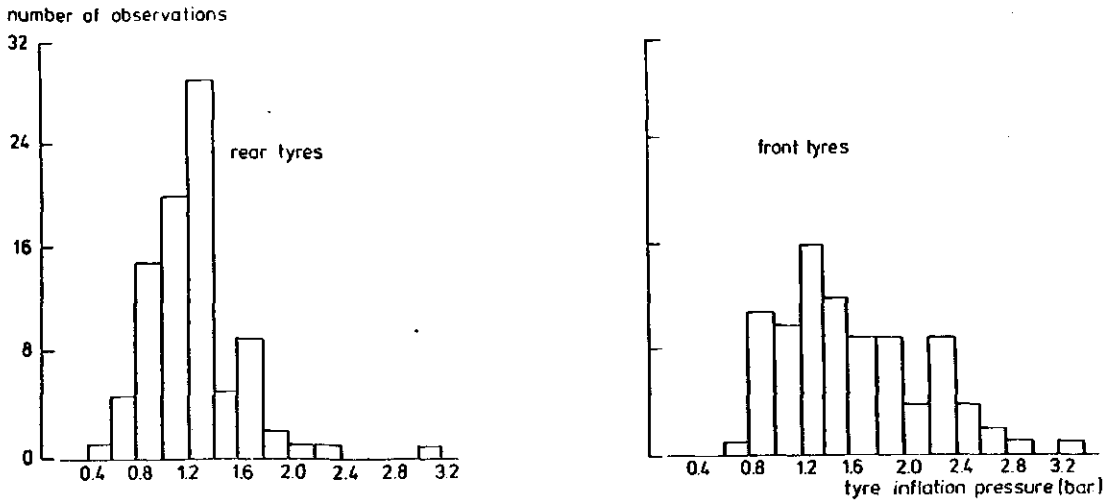

Fig. 3.8. Distribution of tyre inflation pressure of tractors used when ploughing

pressure is between 0.8 and 1.4 bar. Inflation pressure of the front tyres shows a large variation from 0.6 to more than 3.0 bar. 90% is between 0.8 and 2.4 bar, with a rather uniform distribution. It can be concluded that most farmers do not pay as much attention to tyre inflation pressure as they should do. From the viewpoint of physical soil degradation it is important to investigate more quantitatively the significance of the tyre inflation pressure for the soil - wheel interface stresses at different soil conditions.

3.2.3. Wheel-slip percentage

Wheel-slip percentage influences σ_1-distribution in the tyre - soil contact surface, the direction of these stresses, and total backward displacement of the soil in the rut bottom. The last influence is probably the most unknown.

Backward displacement in the rut is always accompanied by pure deformation (change in shape of an elemental soil volume apart from volume change). Physical soil degradation is not only caused by compaction (volume change), but also by pure deformation, which can destroy soil inter-particle bonds. Vehicle designers and users are aware of the detrimental effects of high interface pressures causing severe compaction, but the degradation due to pure deformation is almost totally ignored.

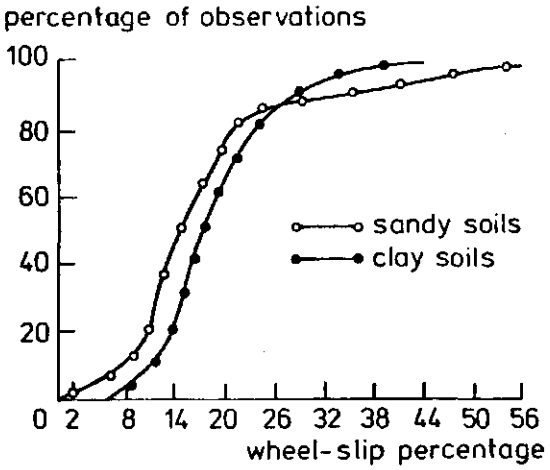

Fig. 3.9. Cumulative distribution of wheel-slip percentages occurring during ploughing

The amount of backward displacement caused by a tyre is, roughly, proportional to the length of the contact surface, and to the slip percentage.

Vehicle designers and extension services recommend optimal slip percentages that entirely stem from maximizing the power efficiency of the vehicle. When tyre dimensions continue to grow, it seems logical that the recommended slip percentage decreases. Data from literature allow the establishment of a relation between tyre size and optimal slip percentage, based on maximum power efficiency. These optimum values range from 10 to 20%, and also depend on soil condition.

To get information on the actual slip percentages in agricultural operations, slip percentages have been measured for 189 tractor-plow combinations on Dutch spring-ploughed sandy soils in spring en clay soils in autumn 1980 (DEN HAAN, 1981; TIJINK en DEN HAAN, 1981). The measured values are plotted cumulatively versus percentage of observations in Fig. 3.9. For both the sandy and clay soils more than 60% of the farmers appeared to plow within the 'good' slip range (between 10 and 20%). It can be seen that measured slip values spread more for the sandy than for the clay soils. The median values (50%) are 14.6% on the sandy, and 17% on the clay soils. The highest slip percentages found are 54% and 37% for the sandy and clay, respectively. On the sandy soils 23% (100 - 77) of the farmers worked at slip percentages higher than 20%. On the clay soils this is even 33%. But the curve for the clay soils shows a steep part beyond the 20% slip point. This means that a small slip decrease would make the number of tractor-plow combinations in the 'good' slip range increase by a large amount. The real high slip values are mainly

due to a bad matching of tractor and plow, and this seems to be more frequent on the sandy than on the clay soils.

When the current idea of optimum slip percentage is used, it can be concluded that too high slip values are exceptional rather than frequent. Improvement can be expected when more attention is paid to matching tractor and plow. This can be promoted by rural extension services. The current idea of optimum slip percentage is purely based on maximum power efficiency. It may be expected that, in the future, this idea will be modified to include also the detrimental effects of high slip percentages on soil structure.

3.3. Some fundamentals on soil deformation

To describe the deformation of a soil, it is often useful to switch from a description in terms of spatial coordinates $\underset{\sim}{x}$ to a description in terms of material coordinates of the solid phase χ_s. In this way many ad hoc models for settlement due to consolidation and/or oxydation of clay, peat, and slurries can be put on a common basis.

For example, the time course of the bulk density ρ_i of a differential volume element of the solid phase can be described by:

$$\rho_i = \rho_{i\kappa}(\det \underset{\sim}{F})^{-1} \exp - \int_{t_\kappa}^{t} (\lambda_i/\rho_i)dt$$

where $\rho_{i\kappa}$ is the bulk density in the reference configuration κ at time t_κ, $\underset{\sim}{F} = \partial x/\partial \chi_{s/t}$ is the deformation gradient tensor of the solid phase, and λ_i is the rate of decay of the solid phase per unit volume. The second order tensor field $\underset{\sim}{F}$ concisely and fully describes the deformation from a reference configuration κ at time t_κ to the configuration at any other time t. In principle $\underset{\sim}{F}$ can be determined by establishing at time t_κ some type of markers of the parcels of the solid phase and determining the locations of these parcels at successive later times. The markers can be some compositional or textural teatures of the solid phase, such as pollen, shells, ash, etc., or they can be purposely inserted objects or material. If attention is restricted to one-dimensional deformation, then the deformation gradient $\partial x/\partial \chi_{s/t}$ can be derived not only from experiments involving markers, but also from the time course of the bulk density profiles of nonreactive constituents.

The theory of mixtures also provides the proper framework for analyzing the forces acting upon the solid phase. Relationships between forces and deformations have been explored to some extent on the basis of an assumption that there exists an internal energy for the soil (RAATS).

3.4. Reports and papers

DAMIAN, T.G., 1983. Some effects of compression and consolidation on soil aggregates at different moisture content levels. Ir. thesis. Tillage Laboratory, Agric. Univ., Wageningen.

HAAN, W.P. DEN, 1981. Wheel-slip during ploughing of clay soils (Dutch). Rep. Tillage Lab., Agric. Univ., Wageningen.

HOFSTRA, S., 1982. Soil compaction in repeated loading (Dutch). Rep. Tillage Lab., Agric. Univ., Wageningen.

KOOLEN, A.J. and H. KUIPERS, 1983. Agricultural soil mechanics. Springer Verlag, Berlin.

RAATS, P.A.C. Applications of the theory of mixtures to the mechanics of soils. In: C. Truesdell (ed.). Rational Thermodynamics, 2nd ed. Springer Verlag, Berlin (in press).

——— Applications of the theory of mixtures in soil science. Proc. 4th Int. Conf. Math. Modelling (in press).

——— The solid phase of a soil: distribution in space and composition (in preparation).

SWINKELS, H.J.M., 1982. Soil air contents during loading (Dutch). Rep. Tillage Lab., Agric. Univ., Wageningen.

TIJINK, F.G.J. and W.P. DEN HAAN, 1981. Wheel-slip during ploughing (Dutch). Landbouwmechanisatie 32,10: 961-964.

4. RESEARCH ON MECHANIZATION, SOIL DEGRADATION AND CROP RESPONSE

4.1. Introduction

To grow arable crops a great amount of field traffic is needed, partly under unfavourable soil conditions. Consecutive field activities after the harvest of a preceding crop are: pre-soil tillage treatments (subsoil loosening in wheel tracks, leveling of the soil surface and incorporation of crop residues), main soil tillage (ploughing, after a potato crop often fixed tine cultivation), fertilization in spring, seedbed preparation, drilling or planting, control of weeds and deseases, ridging of potatoes e.g., fertilization during the growing period (1 or 2 times), spraying schemes, harvest and soil fumigation (in some intensive crop rotations only). The loose soil after the main tillage is subjected to recompaction partly by a natural settlement and partly by field traffic. Especially the first wheel passes after ploughing applied to an often rather wet soil can be very dangerous. In such cases the plane where the pressure exerted by the wheel is in equilibrium with the carrying capacity of the soil is found at a depth of 5 to 10 cm below the surface level created by ploughing.

A practical study carried out on farmers' fields on clayey soils during a period of 23 years revealed not only a considerable variation

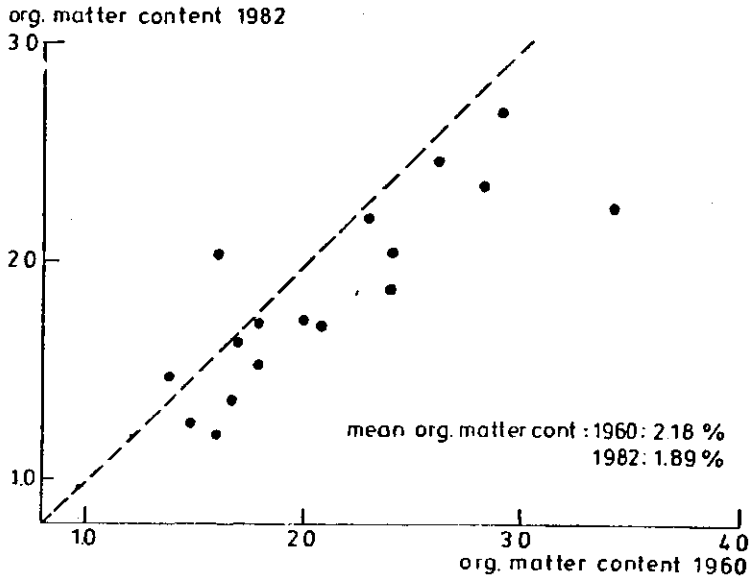

Fig. 4.1. Comparison of organic matter contents in 1960 and 1982 on a number of arable fields in the province Groningen

of the structure of the top layer from year to year, due to changing weather conditions, but also a decrease in soil structure level in the period 1975-1980. The last two years, there was some recovery without reaching the level of years ago. That points to a degradation of the soil structure. This degradation must be attributed to the effect of various factors involved in modern farming. One factor is the more severe compaction due to the use of heavier equipment often under less favourable conditions. Another factor might be the decrease in organic matter content of the top soil (Fig. 4.1). This decrease is not caused by a lower organic matter supply but mainly by deeper ploughing of the soil (BOEKEL, 1982).

4.2. Comparison of soil management systems

To get information about the traffic intensities to which the soil is subjected when growing different crops the next three soil tillage systems have been compared in a crop rotation of consecutively potatoes - winterwheat - sugarbeet and spring barley on an experimental field (LUMKES, 1985).

System A - loose soil husbandry: ploughing each year 25 cm (in autumn), seedbed preparation and drilling or planting in one pass (if possible combined with N-fertilization); for winterwheat ploughing and drilling in one pass

System C - rational tillage (most near to practice): ploughing 15-20 cm for potatoes, 25 cm for sugarbeet, cultivating 15-25 cm with a fixed tine cultivator for cereals; for winterwheat cultivating and drilling in one pass

System B - minimum tillage. No main tillage

System A intended to maintain the soil structure after ploughing looser than system C by combining different field activities. Within 3 m wide strips, the minimum width on which all field traffic except spraying fitted, all the field traffic occurring in practice for potatoes, winterwheat, sugarbeet and spring barley has been registered on maps. An example of a part of such map is given in Fig. 4.2 indicating the place and width of the wheel passes and the type of field operation for potatoe growing. In addition the weight of tractors and implements used, the inflation pressure and size of tyres, the wheel - soil contact sur-

Fig. 4.2. Field traffic pattern for growing potatoes for the three soil tillage systems applied in the experimental field

Table 4.1. Traffic intensity as the cumulative percentage of the soil touched by wheels in field operations needed to grow different crops

		Tillage system		
		A	C	B
Potatoes	main soil tillage	40	29	-
	plantbed preparation, planting + ridging	49	87	87
	harvesting	68	68	68
	total	157	184	165
Sugarbeet	main soil tillage	40	40	-
	seedbed preparation + drilling	49	56	83
	crop control + harvesting	214	214	214
	total	303	303	297
Winter wheat	shallow soil tillage + main soil tillage	69	78	78
	drilling	17	17	17
	crop control + harvesting	48	48	48
	total	134	143	143
Spring barley	shallow soil tillage + main soil tillage	69	58	29
	drilling	49	49	49
	crop control + harvesting	48	48	48
	total	166	155	166

face of each wheel pass and some soil properties were measured. When each pass of a wheel should give a new rut Table 4.1 shows that depending on the type of crop 150 to 300% of the field is covered by ruts.

To reduce the traffic intensity wider implements or a so-called bed culture can be practiced. In a field experiment soil behaviour and crop response of beds free from any traffic have been studied in comparison with normal traffic for a crop rotation potatoes - sugarbeets. The beds had a width of 3.0 m and were separated by 0.3 m wide permanent

Table 4.2. Pore and soil air fractions at pF = 2 under differently trafficked strips on a sugar beet field on clay soil

Depth (cm)	2-7	12-17	22-27	32-37	42-47
Number of passes					
pore fraction					
0	0.576	0.587	0.565	0.472	0.514
2	0.570	0.557	0.510	0.487	0.488
5	0.490	0.455	0.465	0.487	0.518
air fraction at pF = 2					
0	0.282	0.291	0.232	0.129	0.094
2	0.257	0.222	0.130	0.100	0.117
5	0.143	0.079	0.074	0.120	0.098

traffic lanes. All field traffic was restricted to the permanent lanes by adapting wheel distances and implements to bed-width leaving 91% of the area free from any traffic. If each wheel pass should give a new rut such as supposed in Table 4.1 each spot on the fields with normal traffic has been touched by wheels about 4 times in the case of potatoes and about 3 times for sugarbeets. On fields with normal traffic there are strips hardly trafficked and others which are frequently touched by wheels. Table 4.2 compares for a sugar beet field on clay soil pore and soil air fractions with depth from strips without traffic and strips subjected two respectively five times to wheel passes originated from seedbed preparation respectively drilling, spraying and hoeing. Although the field work was carried out under ideal or acceptable soil moisture conditions still a considerable soil compaction was observed.

On the fields with bed culture 91% of the area is free from any traffic and must have ideal soil physical conditions for crop growth. During the experiments several soil physical aspects of the traffic lanes as well as of the beds have been studied applying a sampling scheme as given in Fig. 4.3. The sampling results have been summarized in Table 4.3.

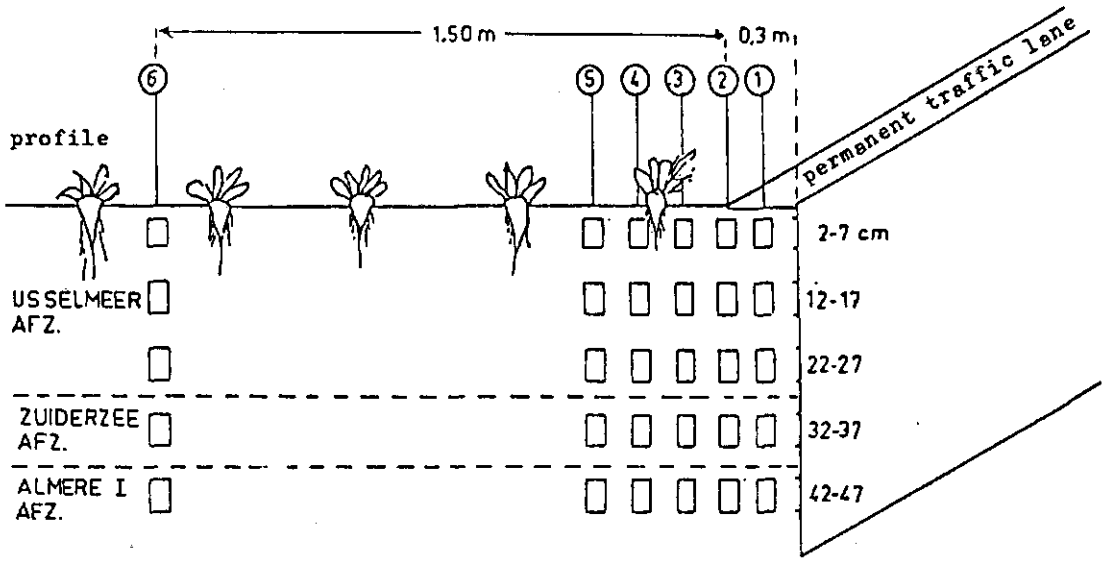

Fig. 4.3. Soil sampling scheme applied to investigate the effect of controlled traffic on soil compaction. The top layer consists of light clay, the subsoil is more sandy

Table 4.3. Pore and air fractions at pF = 2 of the soil in the traffic lane and controlled traffic field

Depth (cm)	2-7	12-17	22-27	32-37	42-47
Spot					
pore fraction					
1	0.485	0.414	0.441	0.497	0.586
2	0.507	0.419	0.448	0.502	0.588
3	0.596	0.452	0.454	0.500	0.593
4	0.536	0.541	0.449	0.510	0.594
5	0.608	0.564	0.508	0.493	0.554
6	0.599	0.570	0.557	0.510	0.470
air fraction at pF = 2					
1	0.115	0.017	0.069	0.123	0.120
2	0.140	0.019	0.074	0.128	0.118
3	0.271	0.074	0.081	0.125	0.123
4	0.217	0.204	0.090	0.121	0.128
5	0.321	0.227	0.147	0.119	0.120
6	0.283	0.233	0.210	0.199	0.137

The spots 5 and 6 reflect the soil conditions unaffected by wheel traffic. Spot 4 on a distance of 45 cm from the centre and 30 cm from the side of the traffic lane shows the influence of the traffic on the lane. The compaction on a depth of 25 cm must be caused by a sidewards movement of the soil under the traffic lanes. In the lane (spot 1 and 2) critical values of pore space and air content are found at depths from about 10 to 30 cm. Also the penetration resistance of the soil in the lanes was very high, 3.5-4.0 MPa, impeding any root growth.

Table 4.4 gives a comparison of the averaged yields of potatoes and sugar beets over the period 1980 to 1982 for fields with normal traffic and beds without any traffic since 1976.

Table 4.4. Potato and sugar yield of fields with normal field traffic and beds with controlled traffic on permanent lanes

Crop	1980	1981	1982
Potatoes			
normal traffic (tons·ha^{-1})	39.2	39.3	37.0
bed culture (%)	109	106	106
Sugar beet			
normal traffic: sugar (tons·ha^{-1})	10.34	11.77	13.32
bed culture (%)	109	102	96

As is demonstrated in Table 4.4 the differences in yield are rather small and positive for bed culture, however more for potatoes than for sugar beets. The latter is caused by too a loose seedbed giving problems with regard to germination and first development of the sugar beet plants. With special techniques this can be avoided. The potato variety used was a special one, more adapted to narrow crop rotations but having a rather low yield level.

Although the relations between crop response and field traffic intensity have to be studied more in detail the data in Table 4.4 indicate that the extra yield obtained by applying bed culture compensates hardly the 9% land loss due to permanent traffic lanes.

4.3. Field traffic and soil compaction in practice

4.3.1. Traffic intensity and frequency

In addition to the experimental soil management systems described in Section 4.2 information has been gathered about traffic intensity and frequency in normal arable farming practice. Also it is tried to find a relation between mechanization degree and soil compaction (VAN DE ZANDE, 1983).

Supposing a coherence between farm size and mechanization degree 27 arable farms have been selected on basis of farm size and texture of the arable layer and subdivided into size categories of <35, 35-55, 55-80 and >80 ha with one farm of 1300 ha. Within these categories distinctions have been made with respect to the texture of the arable layer: 10-15, 15-25, 25-35, 35-45 and more than 45% of the particles smaller than 16 µm.

To characterize the degree of mechanization it appeared not possible to find a parameter including both wheel load, inflation pressure and size of tyres as well as traffic frequency, all factors affecting soil compaction. According to Fig. 4.2 it was tried to visualize conveniently the mechanization degree by mapping the totality of field traffic needed for growing a crop in the form of rut patterns. To this end on the selected farms a complete inventory of implements used for cultivation of the various crops has been made. Of each implement working (wheel) width, dimensions and inflation pressure of tyres and weight were measured. Then per farm a number of parcels has been selected. In close consultation with the farmer the succession of all field operations over the period from ploughing after the harvest in 1980 up to March 1983 was reconstructed for each of these parcels. Per single operation data on time and conditions, type of implement or combination of implements and working depth were collected.

To reconstruct afterwards the rut pattern from these data a computer programme has been developed. In this programme a strip of land in width of the boom length of a sprayer used for plant protection (the implement with the broadest working-width: 24 m) was assumed to comprise all other activities during cultivation of a crop and thus to be representative for all what happens over the entire parcel. From the right edge the strip is filled up with wheel passes, accounting for working-

width, wheel distance, tyre-width both of single and twin tyres. This was done for all successive cultivation activities from ploughing after the former crop up to the harvest of the crop considered. In this way all ruts originated from field traffic needed to grow a crop could be located. Moreover to each rut information about load and inflation pressure of the wheels is attached by using codes. From such computerized rut patterns type of wheel passes in terms of wheel loads and inflation pressures, traffic intensity and frequency can be read simultaneously. With traffic intensity is meant the summed area touched by wheels (in ha) per hectare of land per crop per year. To obtain the traffic frequency the strip is subdivided in separate 10 cm strips. For each 10 cm strip the number of times is counted that the strip is subjected to wheel traffic over the entire cultivation period of a crop.

To investigate the influence of mechanization on soil compaction, on each selected parcel the penetration resistance up to a depth of 70 cm was measured with a penetrograph (cone: top apex 60°, base 1 cm^2). The measurements were carried out in tenfold at an oblique angle (45°) with the direction of field operations. In addition to the penetrometer readings bulk density was measured in sixfold in four layers of 10 cm directly below the arable layer. Per farm size category two parcels were cored, one in the texture category of 15-25% and the other in the category of 25-35% particles <16 µm.

Fig. 4.4 shows an example of a simulated rut pattern originated from field operations successively needed to grow potatoes on a farm larger than 80 ha. The figure gives for strips of 10 cm width information about distribution and width of ruts but also about wheel loads (upper part) and tyre inflation pressures (middle part). The lower part of the figure shows the traffic frequency distribution over the field. To indicate wheel loads and tyre inflation pressures the following codes were used:

Code	A	B	C	D	E	F	G	H
Wheel load (kg)	0-500	-1000	-1500	-2000	-2500	-3000	-3500	-4000

	O	P	Q	R
	-4500	-5000	-5500	-6000

Code	0	1	2	3	4	5	6	7	8	9
Tyre inflation pressure (bar)	0.5-1.0	-1.5	-2.0	-2.5	-3.0	-3.5	-4.0	-4.5	-5.0	-5.5

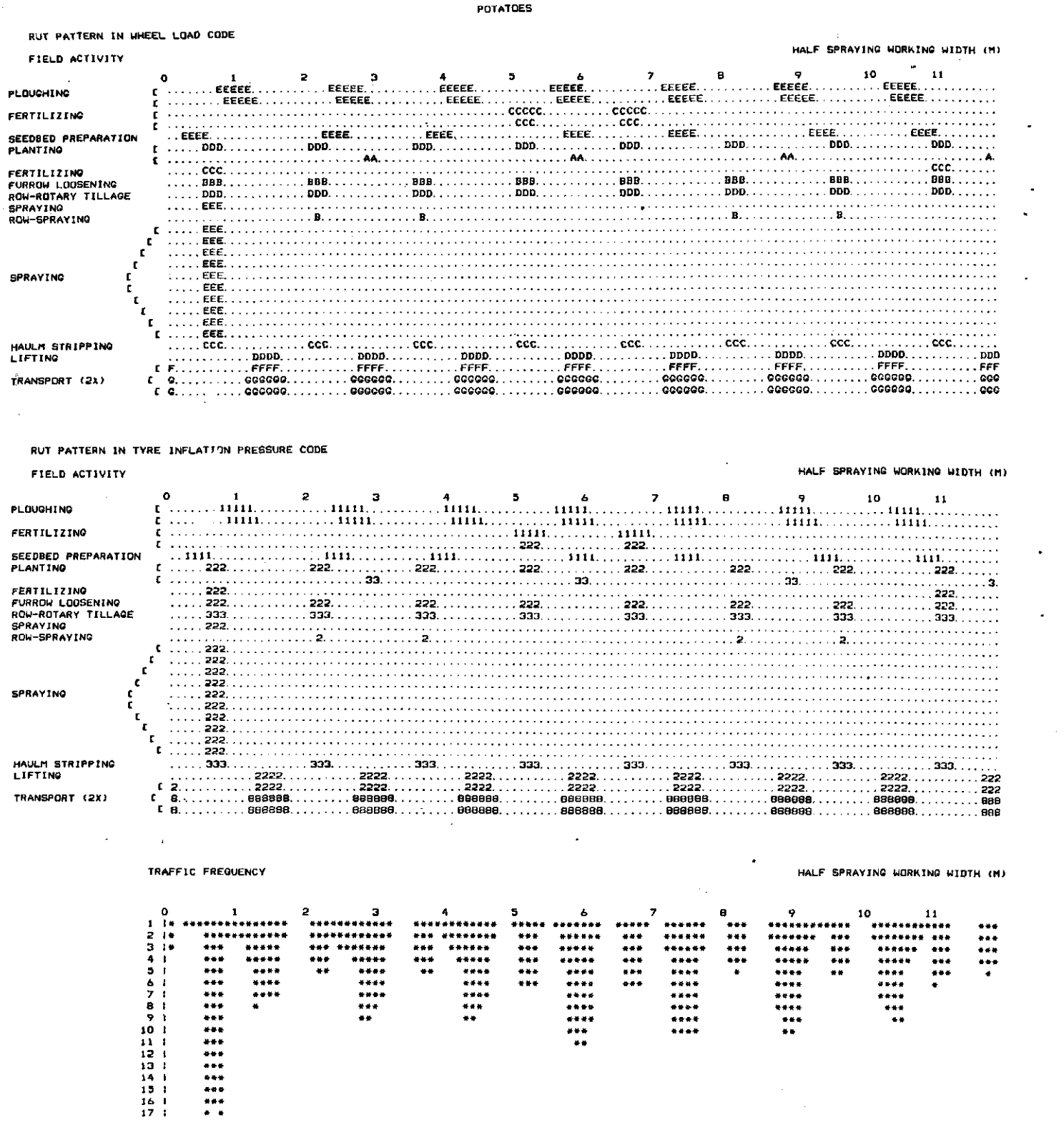

Fig. 4.4. Computerized map indicating intensity in terms of wheel loads and tyre inflation pressure (upper part) and frequency of field traffic needed to grow potatoes on a farm larger than 80 ha

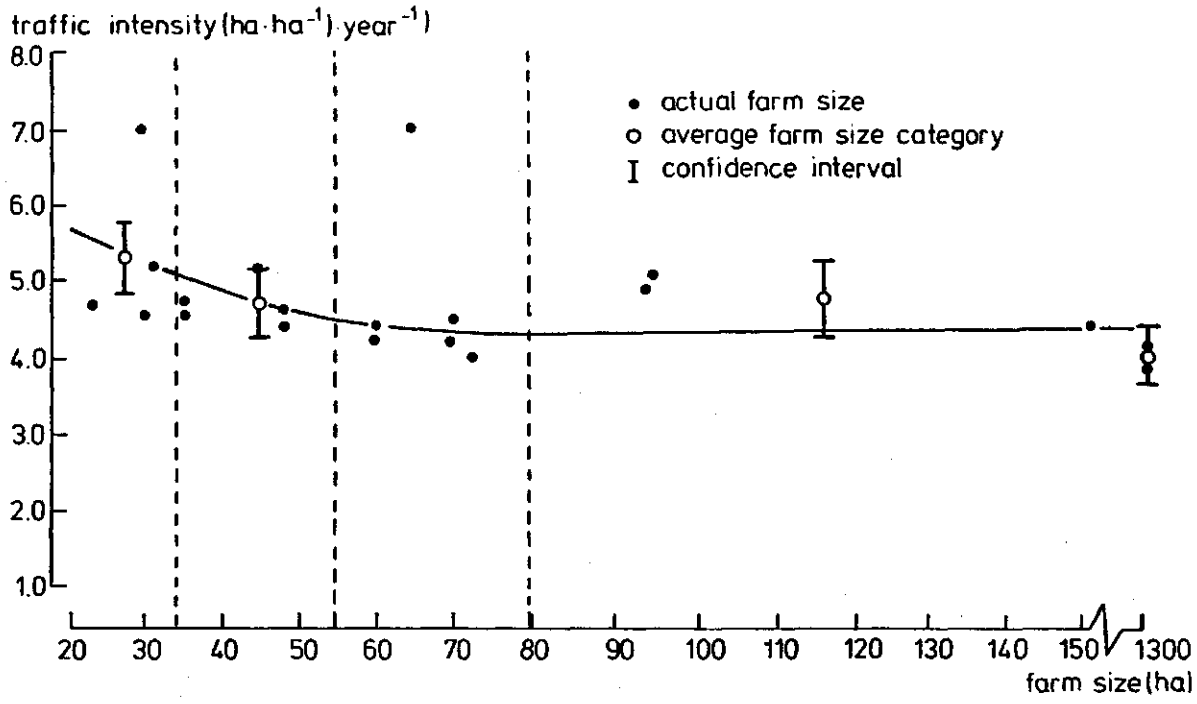

Fig. 4.5. Relationship between traffic intensity and farm size occurring on potato fields

The figure shows that some strips on a potato field are subjected to wheel traffic very frequently. The ruts made by the spraying machine coincide with ruts from other field operations and are touched by wheels about 14 times. Strips where ruts from ploughing and harvesting are situated have been subjected to wheel traffic about 9 times. From data as presented in Fig. 4.4 the traffic intensity can be calculated. This is done for all farms involved in the investigation and for the crops winter wheat, sugarbeets and potatoes. Fig. 4.5 presents the relationship between traffic intensity and farm size for potato cropping. The traffic intensity indicates the summed area touched by wheels (ha) per hectare of land per year. The traffic intensity decreases with increasing farm size. The differences of traffic intensity between the farm size categories <35, 35-55 and 55-80 ha appeared to be significant at 95% confidence. The traffic intensity on the farm of 1300 ha did not differ significantly from that of farms >80 ha, but differed significantly from that of farms <80 ha. Field operations that contribute predominantly to traffic intensity are ploughing, potato-lifting and transport. With increasing farm sizes the working width of plows increases and the potato harvesters used change from 1 row to 2 row lifters. The transport lorries change from one-axle and small biaxial ones on farms <50 ha to bigger tandems with greater tyre widths on the larger farms. Table 4.5 summarizes traffic intensities in relation to farm size.

Table 4.5. Traffic intensity in ha/ha/year and farm size for an averaged crop rotation and the single crops winterwheat, potatoes and sugarbeets (VAN DE ZANDE, 1983)

Farm size (ha)	<35	35-55	55-80	>80
Averaged crop rotation	3.84±0.52(a)	3.47±0.34(ab)	3.26±0.37(b)	3.29±0.13(b)
Winterwheat	2.77±0.49(a)	2.62±0.29(ab)	2.15±0.33(c)	2.21±0.35(c)
Potatoes	5.37±0.57(a)	4.73±0.20(b)	4.37±0.20(c)	4.79±0.60(abd)
Sugarbeets	4.26±1.78(a)	3.85±0.46(ab)	4.21±0.63(abc)	3.37±0.48(ad)

Comparing the figures in horizontal direction, there are no significant differences if the lettres between brackets are similar. The table shows a tendency of a decrease in traffic intensity with increasing farm sizes up to 80 ha. From the table appears also the intensification of field traffic when cereals are replaced by root crops requiring more cultivation passes and producing a higher bulk mass inducing a greater need for heavy wheel traffic. When growing root crops the traffic intensity exceeds in practice about two times that usual for cereals.

4.3.2. Mechanization and soil compaction

To characterize the influence of mechanization degree on soil compaction penetration resistances have been measured at 5 cm depth intervals. The penetrometer readings were grouped according to the categories made for farm size and texture of the arable layer. Fig. 4.6 summarizes these measurements. The curves represent minimum and maximum distributions with depth enclosing the 95% confidence interval. When the penetration resistance exceeds a value in order of 25 to 30 $kg \cdot cm^{-2}$ soil density impedes seriously root penetration. Considering Fig. 4.6 this will be the case on many of the parcels investigated. Noteworthy are the sometimes extremely high compaction levels found immediately below the arable layer especially for the texture class of 15-25% particles <16 µm. At heavier textures compaction below the arable layer is less pronounced. High densities in the subsoil below a depth of about 50 cm cannot probably be ascribed to mechanization but more to the way of sedimentary depositing.

The influence of farm size appears from the intervals between

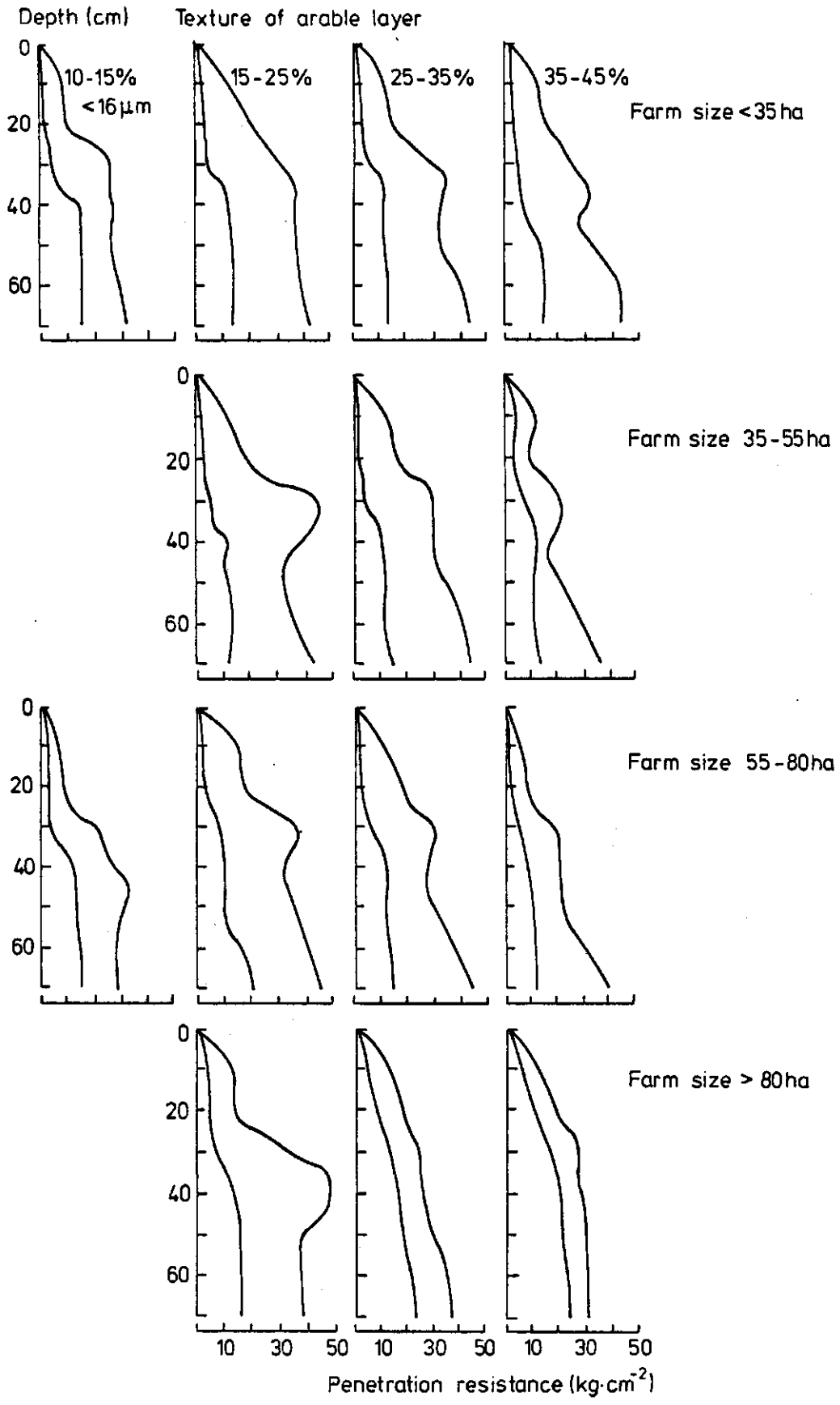

Fig. 4.6. Distribution of the penetration resistance with depth for different categories of soil texture and farm sizes

minimum and maximum curves which become more narrow in cases of larger farm sizes mainly due to a shift of minimum penetration resistances to higher values.

From bulk densities and pore volumes measured on a number of parcels from where also the penetrometer readings originated the same tendencies emerged as found from the penetrometer readings. The layer from about 25 up to 50 cm below surface showed generally the highest density. Moreover the compaction tends to extend to greater depths on farms >55 ha. The latter may be connected with wider tyres applied on larger farms. The mean tyre width of tractors used on farms <35 ha amounts to 35 cm and on farms >80 ha 47 cm. The ground pressure exerted depends on the combination of wheel load, tyre inflation pressure and tyre dimension. Increasing tyre width enlarges the contact surface and reduces the ground pressure, but that pressure is propagated to a greater depth. Soils withstand normally without compaction a mean ground pressure of about 1 bar corresponding with a tyre inflation pressure of about 0.6 to 1 bar. However, most tractors used have tyre inflation pressures varying between 1 and 2.5 bar and transport lorries of 3 to 5 bar (see Fig. 4.4).

In conclusion this development can only lead to more soil compaction to reverse with ever more difficulty because of the increasing depth of occurrence.

4.4. Heavy traffic, soil compaction and production of silage maize

In the Netherlands about 22% (about 150,000 ha) of the arable land is used for growing silage maize, often for years together on the same field. Signals from practice indicate a decrease in yield of silage maize when cropped for years in succession on the same field. A real cause could be physical soil degradation resulting from heavy vehicle traffic. Silage maize is predominantly grown in areas with intensive animal husbandry, mainly occurring in regions with sandy soils. Yearly great amounts of slurry are applied to the maize fields in two or three applications. The weight and capacity of the slurry tankers used are ever more increasing. Wheel loads of 5 to 6 tons become rather usual. Moreover the yield amounts to about 60 tons fresh material, which is harvested and transported with heavy machinery at often wet soil con-

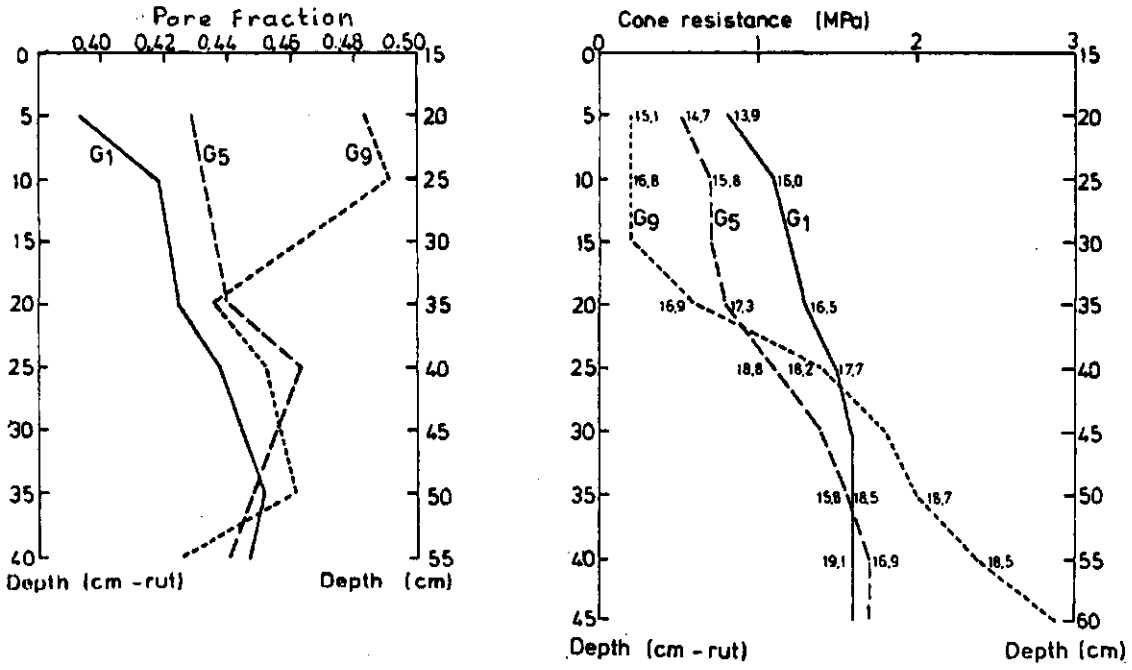

Fig. 4.7. Total pore space and cone penetration resistance as related to depth, 19 and 20 May 1981. G1 = in the rut, G5 = close to the rut, G9 = between ruts. Figures along the curves = moisture content (%, w/w) at sampling

ditions. It is not exceptional that the fresh product is transported from the land with trucks of a total weight of 30 tons.

Measurements of DANIELS, POT and OUWERKERK (1984) on a sandy soil trafficked with a 30 tons slurry tanker under relatively dry conditions after sowing of maize in spring showed a decrease of pore space and increase of cone resistance to a depth of about 20 cm in the soil below and adjacent to the ruts (Fig. 4.7). HAVINGA and BOELS (1982) carried out field traffic experiments and varied wheel loads, tyre inflation pressure and number of wheel passes. Fig. 4.8 gives some results for a sandy soil. At wheel loads up to 6000 kg, not unusual on maize fields, soil compaction extends to depths of 60 to 80 cm when the soil is trafficked more times in succession.

After these introductory experiments two experimental fields were started in autumn 1982 on two different sandy soils (at Westerhoven and Heino) to study the effects of heavy traffic on soil compaction and yield of silage maize, grown for years in succession (VAN DER SCHANS, 1984). The sandy soil at Westerhoven consists of a top layer low in

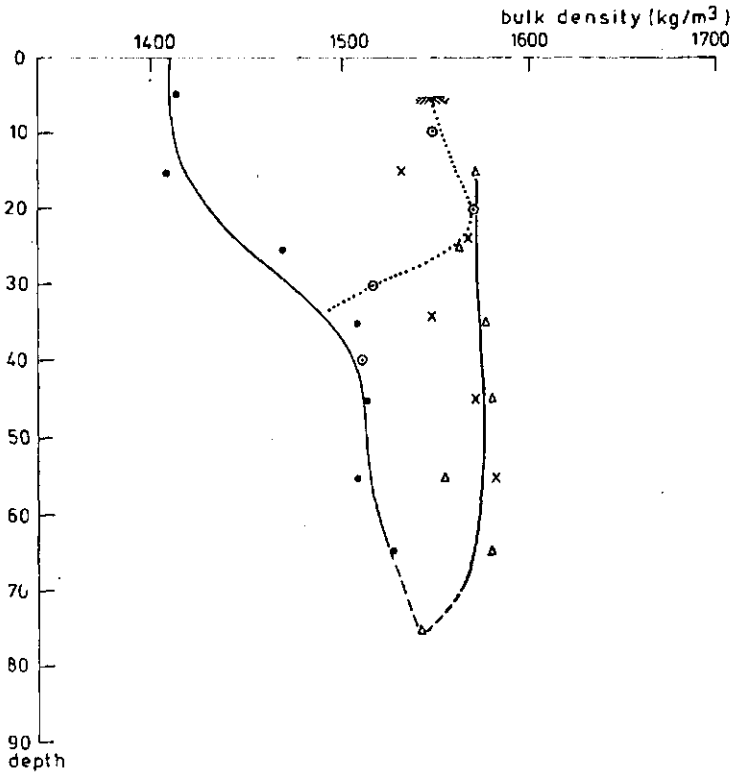

Fig. 4.8. Bulk density distribution with depth for different combinations of wheel loads and wheel passes: . initial bulk density distribution; ⊙ wheel load 1600 kg, 8 passes; x wheel load 3200 kg, 8 passes; Δ wheel load 6400 kg, 6 passes

organic matter content overlying a poor sandy subsoil. The Heino sandy soil consists of a loamy sandy subsoil covered by a 35 cm humous sandy top layer. On each experimental field the next three treatments have been realized in fourfold:

A: entire field trafficked with 6 tons wheel load
B: entire field trafficked with 2 tons wheel load
O: controlled field traffic

Although the treatments are initially more extreme than the mean situation in practice, they can be considered, however, to be representative for fields trafficked with heavy vehicles year after year, occurring on many of the fields in use for growing maize.

The treatments A and B decreased the pore fraction to values smaller than 0.40 at which sandy soils become too dense for rooting. This com-

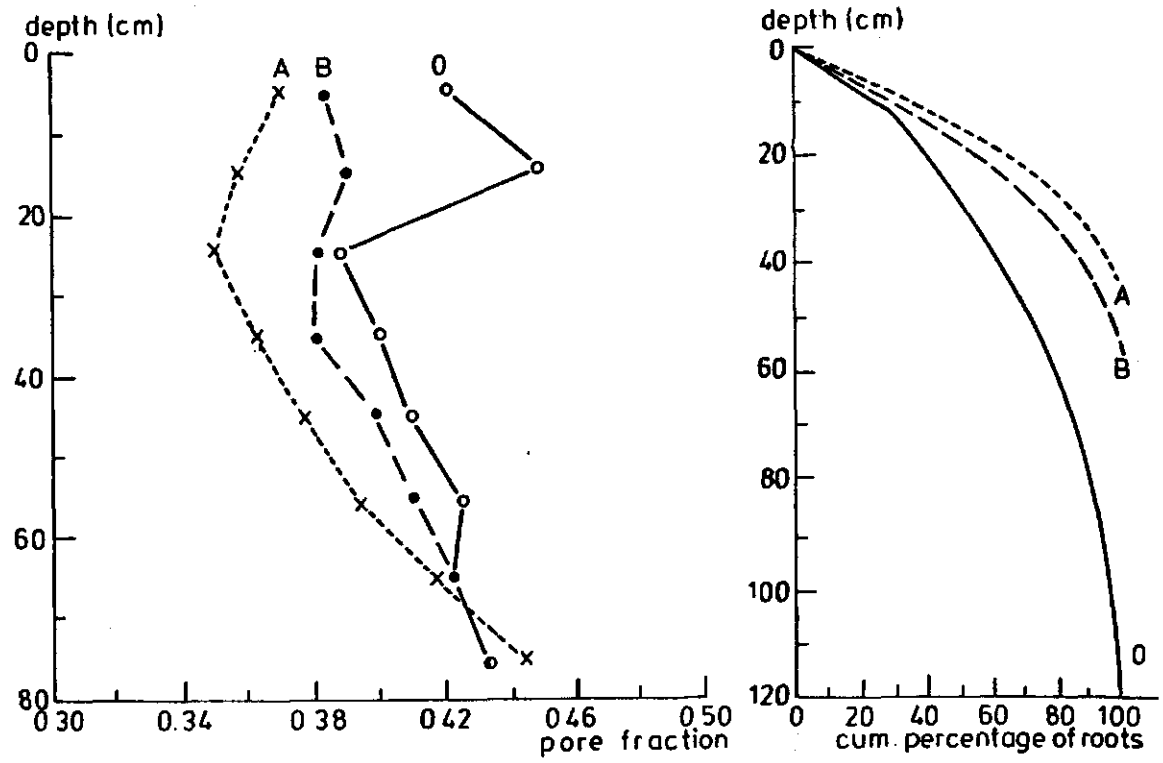

Fig. 4.9. Distribution with depth of pore fraction and cumulative percentage of roots in the Westerhoven sandy soil when trafficked with wheel loads of 6000 kg (A), 2000 kg (B) and at controlled traffic (0)

paction occurs to a depth of 50 to 70 cm and impedes root propagation to deeper soil layers (Fig. 4.9). Root growth was restricted to the upper 40 to 50 cm on the heavely trafficked fields. On the untreated field the rooting depth amounted to 130 cm.

Compaction of the subsoil and restriction of the rooting depth reduced considerably the yield of silage maize in 1983 (Table 4.6).

Table 4.6. Dry matter yield (tons·ha^{-1}) of silage maize at Westerhoven and Heino in 1983

Treatment	Westerhoven	Heino
A: wheel load 6 tons	11.9 (66.5%)	13.1 (90.9%)
B: wheel load 2 tons	15.9 (88.8%)	12.4 (86.1%)
0: controlled traffic	17.9 (100 %)	14.4 (100 %)

The yield depression after heavy traffic is mainly caused by a restriction of water supply to the roots from the subsoil due to a

shallow root depth. This negative effect depends to a large extent on the weather conditions in the growing season and will be the greatest in dry years. This argues to continue these experimental fields over a longer period

4.5. Soil degradation and activity of roots

In research concerning the influence of physical soil degradation on crop yield, rooting and root activity play an important role. Root development can be restricted by a high mechanical resistance and an unsufficient aeration of the soil or in parts of the soil (clods). This leads to a limited availability of nutrients.

In a theoretical study the role and significance of partial blocking of the root surface by a soil aggregate with respect to oxygen supply and the importance of limited contact between soil and root with respect to supply of nutrients was examined (Fig. 4.10). It appears that for mobile ions like nitrate, even when contact between root and soil is very much restricted, transport to the root can proceed at the re-

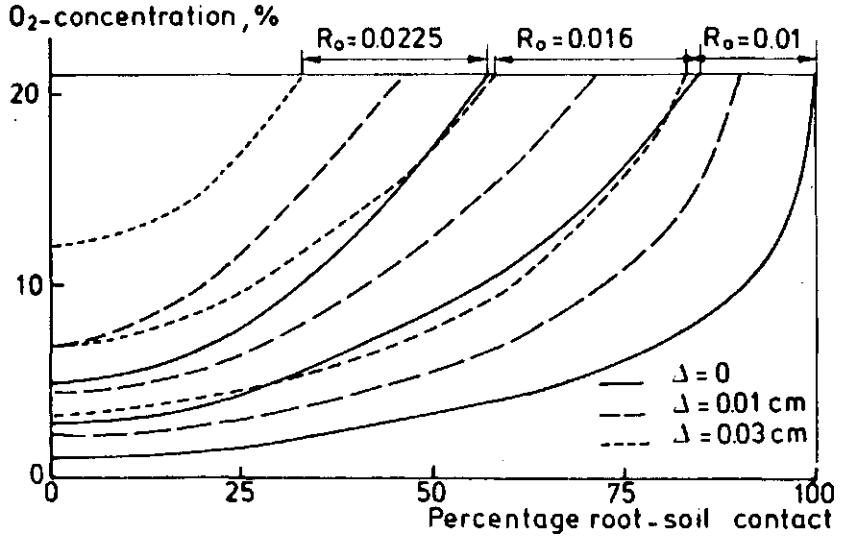

Fig. 4.10. Percentage oxygen pressure in soil air required to keep all parts of the root in aerobic condition as a function of percentage of root - soil contact for 3 values of root radius (R_o,cm) and 3 values for the thickness of the waterfilm (Δ) covering the part of the root in contact with pores. An increased contact (e.g. in more compact soil) increases the oxygen pressure required

quired rate. For strongly adsorbed ions like phosphate the situation is more complicated. If roots are in partial contact with the soil, a higher root density is required for phosphate uptake than in case of complete contact. This increase is probably less than proportional to the decrease in contact, but some of the physiological assumptions underlying this conclusion remain uncertain (DE WILLIGEN and VAN NOORDWIJK, 1984; VAN NOORDWIJK and DE WILLIGEN, 1984).

4.6. Effect of drainage and soil compactability

More than 60% of the arable land in the Netherlands is used for growing potatoes, sugarbeets and silage maize. These crops produce great bulk masses which are harvested in the period September - October. The wetter the soil, the more susceptible to compaction. To prevent compaction, one has to reduce wheel loads or to realize a drier soil or both.

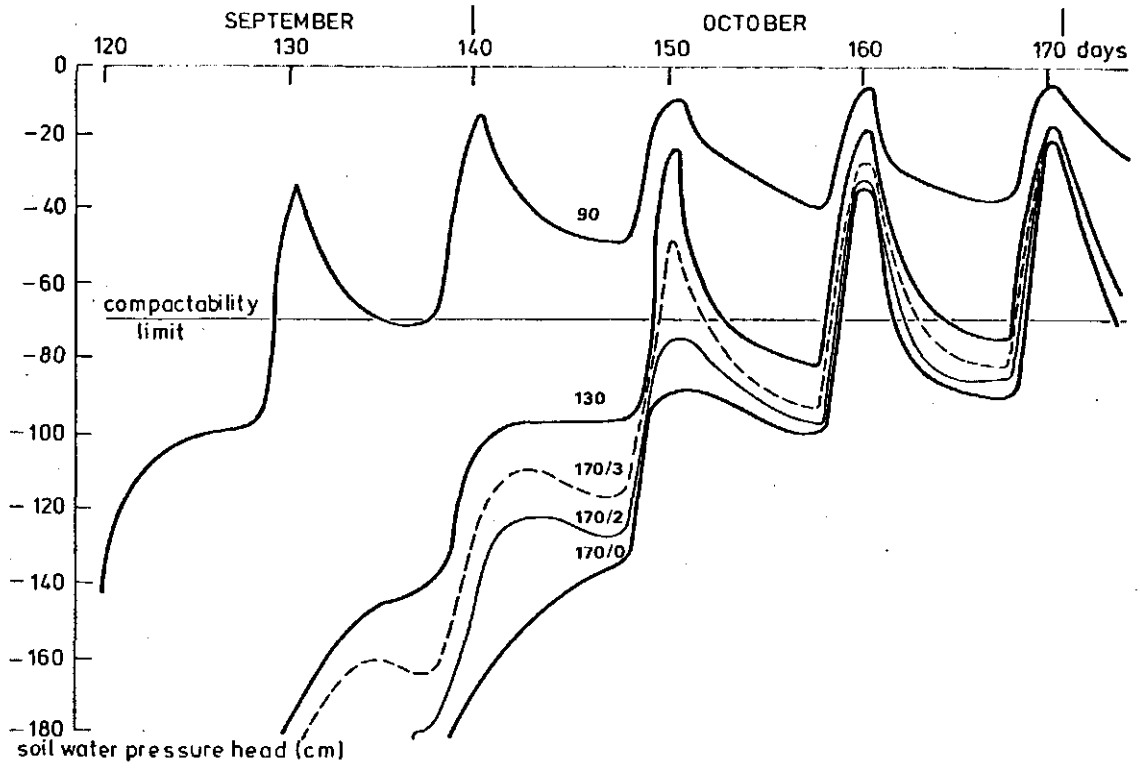

Fig. 4.11. Simulated course of the pressure head at 30 cm depth in a sandy soil after a schematized rainfall pattern in September and October for drain depths of 90, 130 and 170 cm. The drain depth of 170 cm is combined with a supplemental water supply of 0 (170/0), 60 (170/2) and 90 mm (170/3)

The moisture content of the soil in autumn is mainly determined by the weather conditions in autumn as well as by those in the preceding summer. In addition drainage and water supply, if any, will influence soil moisture conditions and in this way soil compactability.

To quantify the extent to which drainage and water supply during the preceding summer affect the compactability of the soil a model research has been carried out (WIND, 1984). To this end an existing and approved model has been used simulating soil moisture conditions in dependency of soil physical properties, rainfall and drainage conditions. Starting with a moisture depletion of the soil of 150 mm on September 1 a schematized rainfall pattern was applied consisting alternately of eight dry days followed by two days with 15 mm of rain each. The soil considered was a sandy soil which is susceptible to severe compaction at pressure heads >-70 cm. Fig. 4.11 shows the simulated course of the

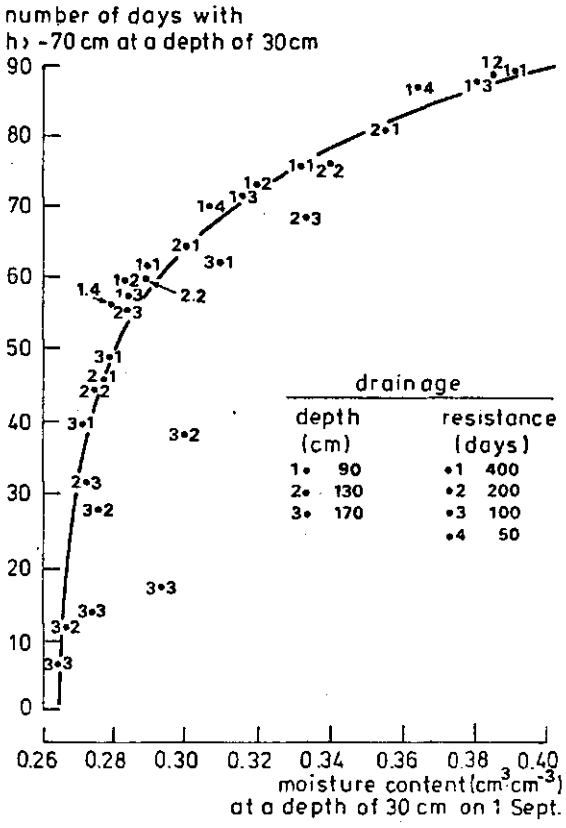

Fig. 4.12. Summed number of days on which the soil water pressure head limit for compactability of a sandy soil (h $\geq$-70 cm) is exceeded versus the soil moisture content at the end of the preceding summer for three drain depths, four drain resistances and three different summers (dry, normal and wet: each figure combination occurs three times in the figure)

pressure head on a depth of 30 cm for drain depths of 90, 130 and 170 cm.

At a drain depth of 90 cm the soil is severely compactible from September 20 continuously. At drain depths of 130 and 170 cm the compactability limit is exceeded first on October 9 and 18 respectively. Moreover at these latter drain depths the soil water pressure head falls below the compactability limit during dry periods. During this schematized autumn the subsoil was not susceptible to compaction during 10, 42 and 48 days for drain depths of 90, 130 and 170 cm respectively.

In this context drainage is double-acting: preventively as well as curatively. A deeply drained soil is drier at the beginning of the autumn than a shallowly drained soil. The curative effect of a good drainage consists of a faster discharge of water excess. The model calculation showed that the preventive effect exceeds the curative one (Fig. 4.12). It appeared that the soil moisture content at the beginning of the autumn accounts for 80% of the differences in the number of days on which the soil is susceptible to compaction. Moreover the curative effect is only found at great drain depths.

A conclusion from this model research could be that some yield depression due to drought has to be accepted to prevent physical soil degradation due to wet soil conditions during harvest in autumn. In fact this requires supplemental research that quantifies the present yield depressions as well as the futural yield losses due to soil compaction.

4.7. Reports and papers

BOEKEL, P., 1982. Soil structure in modern agriculture. Proc. 9th Conference of the Intern. Soil Tillage Research Organization, Osyek 1982.

DANIËLS, D., D. POT and C. VAN OUWERKERK, 1984. Soil structure deterioration of a sandy soil caused by trafficking with a heavy slurry tanker. Research on field experiment PAGV 689 at Borkel en Schaft (near Valkenswaard) in 1981 (Dutch, with English summary). Rapport -84 Instituut voor Bodemvruchtbaarheid (in press).

HAVINGA, L. and D. BOELS. 1982. Compacting of a sandy soil due to different wheel loads (Dutch). Nota ICW 1388. 40 p.

LUMKES, L.M., 1985. Applied traffic research in arable farming and field production of vegetables by PAGV in the Netherlands. Proc. Int. Conf. on Soil Dynamics, Auburn, Alabama (in preparation).

NOORDWIJK, M. VAN and P. DE WILLIGEN, 1984. Mathematical models on diffusion of oxygen to and within plant roots with special emphasis on effects of soil - root contact. II. Applications. Plant and Soil 77: 233-241.

SCHANS, D.A. VAN DER, 1984. Heavy traffic, soil compaction and yield of silage maize (Dutch). De Buffer 30,1: 7-18.

WILLIGEN, P. DE and M. VAN NOORDWIJK, 1984. Mathematical models on diffusion of oxygen to and within plant roots with special emphasis on effect of soil - root contact. I. Derivation of the models. Plant and Soil 77: 215-231.

WIND, G.P., 1984. Drainage and soil compactability (in preparation).

ZANDE, J. VAN DE, 1983. Field traffic and compaction of arable soils in West-South-Beveland (Dutch). Nota ICW 1462. 56 p.